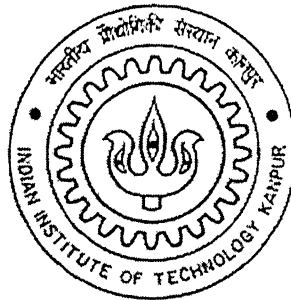# STATIC SYNCHRONOUS SERIES COMPENSATOR (SSSC) BASED DAMPING CONTROLLER FOR DAMPING OUT LOW FREQUENCY OSCILLATIONS IN A POWER SYSTEM

A thesis submitted
in partial fulfillment of the requirements
For the degree of

MASTER OF TECHNOLOGY

by

K. Kiran

to the

Department of Electrical Engineering
INDIAN INSTITUTE OF TECHNOLOGY, KANPUR
August 2005

CERTIFICATE

This is to certify that the work contained in this thesis entitled **"STATIC SYNCHRONOUS SERIES COMPENSATOR (SSSC) BASED DAMPING CONTROLLER FOR DAMPING OUT LOW FREQUENCY OSCILLATIONS IN A POWER SYSTEM"**, by **K. Kiran, Roll No: Y3104043** has been carried out under our supervision and that this work has not been submitted elsewhere for any degree.
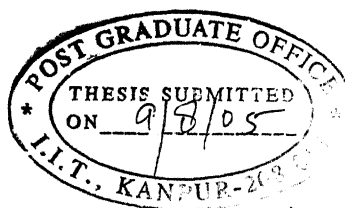
Dr. Sushil Kumar Agrawal

Addl. General Manager,

Power Grid Corporation Of India Limited

New Delhi.

Dr. Shyama. P. Das

Associate Professor

Department of Electrical Engineering

Indian Institute of Technology

Kanpur, India

July 2005

ACKNOWLEDGMENTS

Dedicated to my parents

ABSTRACT

As an interconnected power system is subjected to a large load with rapid change, system frequency may be severely disturbed and become oscillatory. To stabilize the low frequency oscillations, the dynamic power flow control of static synchronous series compensator (SSSC) located in series with transmission lines is required. With the system power flow through the transmission line taken as the control variable, the power flow control by an SSSC in a transmission system creates a sophisticated method of frequency stabilization.

This thesis presents a systematic approach for designing a static synchronous series compensator (SSSC) based damping controller using phase compensation method for damping out low frequency oscillations in a power system. The selection of the operating point for designing damping controller for robust performance to variations in system loading and system parameters has also been attempted. Detailed investigations have been carried out considering two alternative SSSC based damping controllers. The investigation reveals that for the damping controller based on SSSC parameter 'δ_b' (Phase angle of inverter output voltage) provides superior performance to variations in system loading and system parameters compared to damping controller based on SSSC parameter 'm' (Inverter amplitude modulation index). The proposed method of designing SSSC based damping controller is also applied to a part of Indian transmission system.

Key words: *SSSC, damping controller, three-level inverter, Indian transmission system.*

CONTENTS

5. Conclusions

List of Figures

List of Symbols

$V_c(\alpha)$	Voltage across capacitor as function of firing angle α.
$I_L(\alpha)$	Current through inductor.
Vq	Series injecting voltage.
X_c	Capacitive reactance.
X_L	Inductive reactance.
V_a	R phase voltage output of PWM multi bridge inverter.
T_1, T_2, T_3, T_4	Carrier signals each displaced by 90°.
r_b	Equivalent circuit resistance of SSSC.
l_b	Equivalent circuit inductance of SSSC.
$I_{l.a}$	R Phase line current.
δ_b	Phase angle of output voltage of inverter or dalay angle of three level multi bridge PWM inverter.
$G_p(s)$	Transfer function of system.
$G_c(s)$	Tranfer function of controller.
m	Amplitude modulation index of PWM inverter.
σ	Tranformation ratio of coupling transformer.
V_{dc}	Magnitude of D.C link voltage.
k	Fundamental a.c to D.C gain factor.
X_{ref}	Compensating reactance demand.
V_{dc}^{*}	Reference D.C capacitor voltage.
P	Park's transformation.
X_{SCT}	Reactance of the coupling transformer.
ω_b	Angular frequency in rad/sec.
E_{fd}	Voltage proportional to field voltage.
P_m, P_e	Mechaniclal and Electrical power respectively.
T	Time constant.
x	State variable.
u	input variable.

Prefix Δ denotes change in value (Increment / Decrement).

Superscript ' denotes transient.

Subscript d,q,o denotes d-q-o axis variables.

A dot over symbol denotes differentiation w.r.t time.

Any other symbols used in the text are explained as and when they were introduced.

CHAPTER 1

INTRODUCTION

The growth in the demand for electric power is ever increasing. In countries like India where most of the energy resources concentrated at some places, much of the power generated needs to be transmitted over long distances. Environmental and right of way concerns hinder the construction of new power projects and transmission lines. Therefore the existing lines are required to utilize effectively to evacuate increasing amount of power generated. Static capacitor banks can be used in series with long transmission lines in order to compensate for their large inductive reactance, which would otherwise limit the maximum power that can be transfered down the line. Series capacitor compensation also improves the transient stability and voltage regulation of the system. However, the extent to which a transmission line can be compensated with series capacitance is often restricted by the concerns of the destructive effects of sub synchronous resonance.

Simultaneous growing demand of power and environment concern necessitated a review of the traditional power system concepts and practices to achieve greater operating flexibility and better utilization of existing transmission system. Rapid development of power electronics technology provides exciting opportunities to develop new power system equipments for better utilization of the existing systems. Hingoroni [1] proposed the concept of flexible AC transmission systems (FACTS), which provides the needed correction of transmission functionality in order to fully utilize the existing transmission systems. FACTS technology based on use of reliable high speed power electronics, advanced control technology, advanced micro-computers and powerful analytical tools. This technology has been demonstrated successfully and continues to be implemented at transmission locations in various parts of the world [2]. The installed FACTS controllers have provided new possibilities and unprecedented flexibility aiming at maximizing the utilization of transmission assets efficiently and reliably.

Nowadays, the electric power system is in transition to a fully competitive deregulated scenario. Under this circumstance, any power system controls such as frequency and voltage controls will be served as ancillary services [3, 4]. Especially, in the case that the proliferation of non-utility generations, i.e., Independent Power Producers (IPPs) that do not

possess sufficient frequency control capabilities, tends to increase considerably. Furthermore, various kinds of apparatus with large capacity and fast power consumption such as a magnetic levitation transportation, a testing plant for nuclear fusion, or even an ordinary scale factory like a steel manufacturer, etc., increase significantly. When these loads are concentrated in a power system, they may cause a serious problem of frequency oscillations. The convention frequency control, i.e., governor, may no longer able to absorb these oscillations due to its slow response [5]. A new service of stabilization of frequency oscillations becomes challenging and is highly expected in the future competitive environment.

The problem of poorly damped low frequency oscillations associated with generator rotor swings has been a matter of concern to power engineers for a long time. This problem is aggravated due to increased power transfer levels in the transmission network. The traditional solution to the problem is use of Power System Stabilizer (PSS). In addition, HVDC, SVC controllers have also been used to damp these low frequency oscillations. The advent of high power electronic equipments to improve the utilization of transmission capacity provides system planners with additional leverage to improve stability of the system.

The SSSC is a Flexible AC Transmission Systems (FACTS) device that has been reported in the literature as an effective apparatus with an ability of dynamic power flow control [6]. This can control power flow through the transmission line by compensating line reactive voltage drop, by modulating magnitude and phase of the compensating voltage. Thus we can control the power flow and provide damping to low frequency oscillations.

1.1 Series FACTS Controllers

It was always recognized that ac power transmission over long distances was primarily limited by series reactive impedance of the line. Traditionally series capacitors are used to cancel a portion line reactance and thereby increase in transmittable power. Subsequently with FACTS initiative, it has been demonstrated that variable compensation is highly effective in both controlling power flow in the line and in improving stability. The development of FACTS controllers has followed two distinctly different technical

approaches, both resulting in a comprehensive group of controllers able to address transmission problems. The first group employs reactive impedances or tap changing transformers with thyristor switches as controlling elements. They include static var compensator (SVC), thyristor controlled series capacitor (TCSC), thyristor controlled phase angle regulator (TCPAR). The second group of controllers employs self commutated voltage sourced switching converters to realize controllable static synchronous ac voltage or current sources. This group of controllers includes static compensator (STATCOM), static synchronous series compensator (SSSC), unified power flow controller (UPFC), interline power flow controllers (IPFC). In addition to these FACTS devices mentioned above, special purpose FACTS devices NGH damping scheme [7], thyristor controlled breaking resistor (TCBR) [8] for stability improvement and thyristor controlled fault current limiter (FCL) [9] are also considered as part of the FACTS family.

Variable compensation facilitates effective utilization of existing transmission assets by controlling the power flow in lines, preventing loop flows and with use of fast controls minimizing the effect of system disturbances thereby reducing traditional margin requirements. The operation of controllable series devices may be explained in terms of injection of voltage in phase opposition to the reactive voltage drop of transmission line. The effect is independent of how the controllable series voltage is created [10]. It may be consequence of the voltage drop across controllable impedance or it may be injected into line using coupling transformer. The main two FACTS series controllers are controlled series capacitor (CSC) and static synchronous series compensator (SSSC). CSC in the form of thyristor controlled series capacitor already exists in India at Ballabgarh and Rourkrela and some other parts of the world.

1.1.1 Controlled series capacitor (CSC)

Controlled Series Capacitor (CSC) is generally in the form of thyristor controlled series capacitor (TCSC) or thyristor switched series capacitor (TSSC) or may be combination of both. General structure of TSSC is shown in Fig 1.1 .It consists of number of capacitors each shunted by an appropriately rated bypass valve composed of string of anti-parallel connected thyristors which acts as bypass switch. The operating principle of TSSC is straight

forward, the degree of compensation is controlled in steps like manner by increasing or decreasing no of series capacitors inserted. Capacitor is inserted by turning off, and it is bypassed by turning on the corresponding thyristor valve. Therefore series compensation in discrete steps is only possible with TSSC.

TCSC consists of compensating capacitor shunted by a thyristor-controlled reactor. by controlling firing angle of anti-parallel thyristors we can change effective inductive reactance of parallel branch, which in turn cancels the portion of capacitive reactance on the series capacitor. The structure of TCSC is shown in Fig 1.2. The TCSC module has three basic operating modes i) Bypassed mode ii) Inserted with thyristor valve blocked iii) inserted with vernier control. In the bypassed mode thyristors are gated for full conduction (180°) and the current flow in the reactor is continuously and is sinusoidal. This mode is mainly for protecting compensating capacitor from over voltages. In the second mode, no current flows through thyristors with blocking of gate pulses. In this case TCSC reactance is same as that of fixed capacitor and there is no difference in the performance of TCSC in this mode with that of fixed capacitor. In the inserted mode with vernier control, the thyristor valves are gated such that thyristors conducts part of cycle ($\alpha_{min} < \alpha < 90^\circ$). The effective TCSC reactance (capacitive region) increases as α is reduced below 90° and the TCSC reactance is maximum when $\alpha = \alpha_{min}$ which may be three times the fixed reactance. This angle α_{min} is slightly above the values of α corresponding to the parallel resonance of thyristor controlled reactor and the fixed capacitor at fundamental frequency.
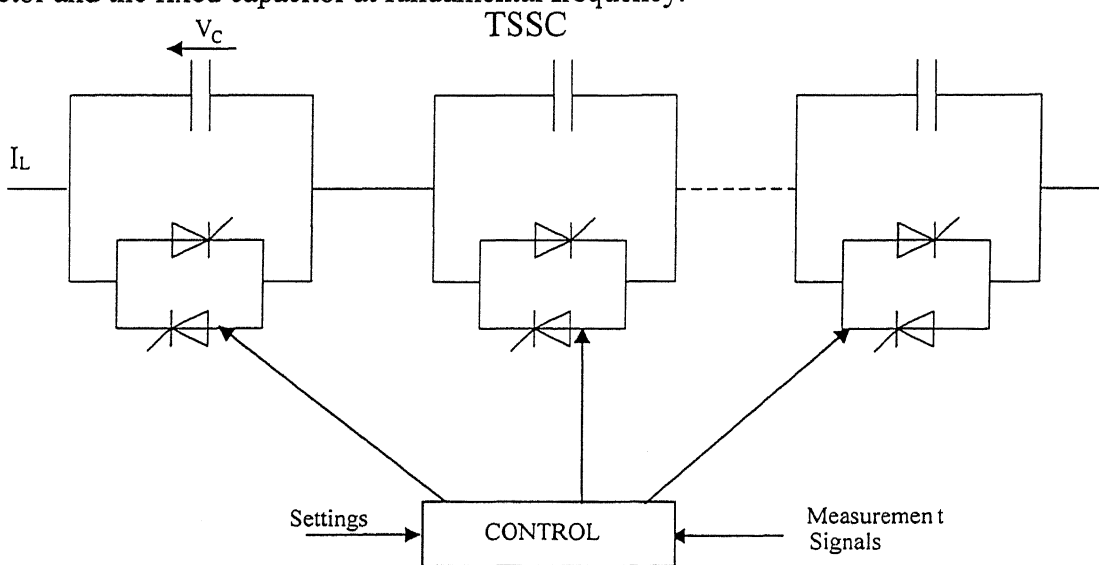
Fig 1.1. General Scheme of TSSC

TCSC

$V_C(\alpha)$

$I_C(\alpha) = I + I_L(\alpha)$

I

$I_L(\alpha)$
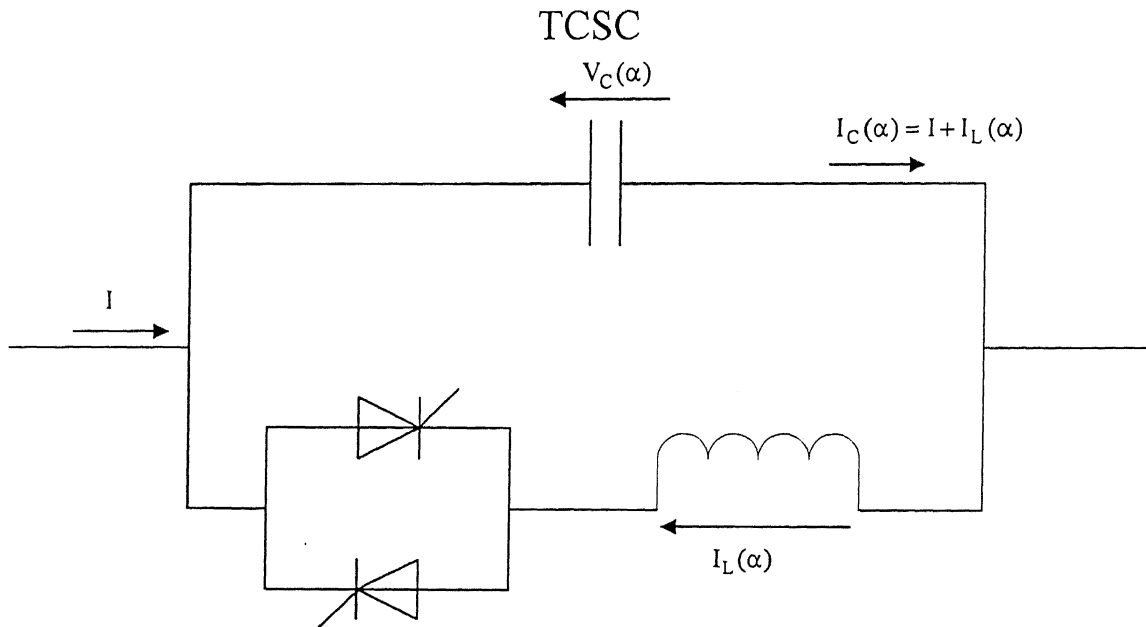
Fig 1.2: Basic thyristor control series capacitor (TCSC) scheme

1.1.2 Static synchronous series compensator (SSSC)

Static synchronous series compensator (SSSC), proposed by Gyugyi [6], is a relatively newer FACTS device. Basic structure of SSSC is shown in Fig 1.3. It consists of coupling transformer to inject voltage in series with line, voltage source converter, DC circuit and controls. Voltage source converter with its internal control can be considered as synchronous voltage source. It can produce three-phase alternating sinusoidal voltages with controllable voltage magnitude and phase angle. The concept of SSSC is same as that of fixed series capacitor that can produce an appropriate voltage at fundamental frequency in quadrature with the transmission line current in order to increase voltage across the inductive line impedance, and thereby increase in line current and transmitted power. Operating characteristics of SSSC differs from CSC. While CSC represents controllable reactive impedance, an SSSC acts as a controllable reactive voltage source whose magnitude can be controlled independent of the line current. CSC can be realised using conventional thyristors, but an SSSC requires semi conductor switches with turn off capability.

5
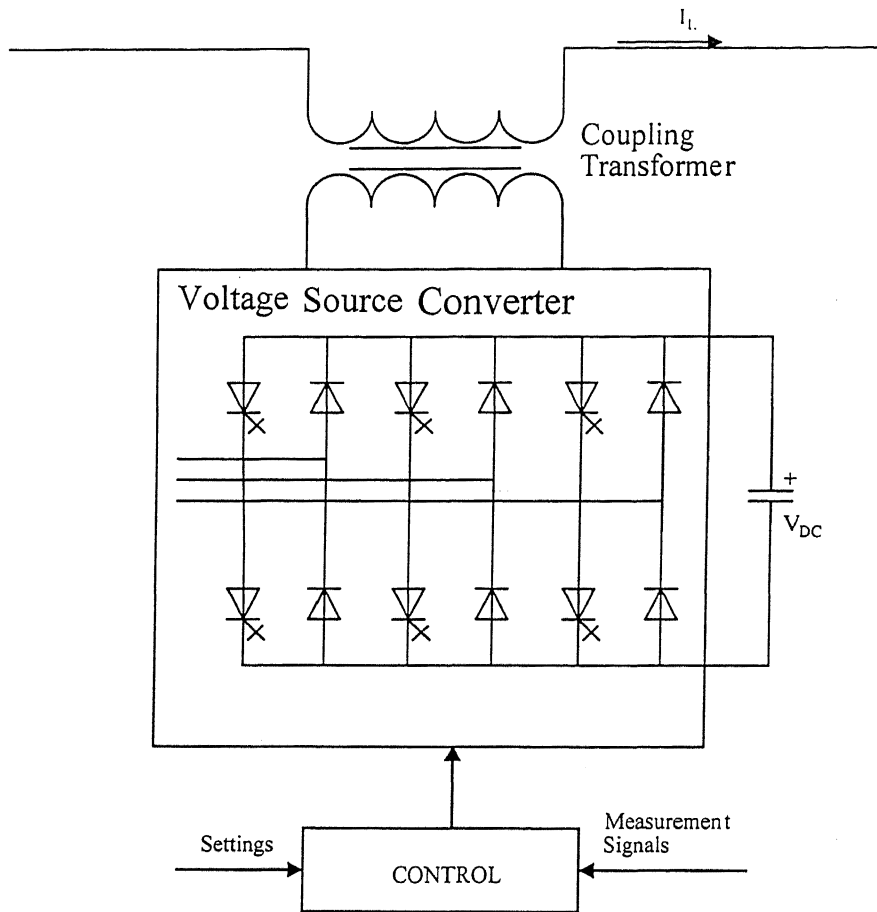
Fig 1.3 Basic structure of SSSC

1.2 Review of Literature

The possibility of switching converters for the generation of reactive power to provide shunt reactive compensation has been realised [11].Initially the effort was focused on shunt compensators. The voltage source converter based series compensator called static synchronous series compensator (SSSC), was proposed by Gyugyi in 1989 [6] with the concept of using converter based technology for shunt and series compensation, as well as for transmission angle control. Subsequently this approach was extended in 1991 to the concept of the unified power flow controller (UPFC) [12] and was generalized for the comprehensive, dynamic control of active and reactive power flow [13,14].

Voltage source converter structures investigated included the three-phase three-level multi-bridge pulse width modulation voltage source converters [15] and Multi-bridge inverters [16]. For high power applications, conventional high pulse schemes utilize phase shifting transformers to combine the output of several two-level inverters. Multi-level voltage

source inverters based on GTO thyristors are capable of harmonic performance equivalent to conventional high pulse schemes based on two-level inverter. The output of Multi-level inverter can be computed to eliminate a number of low order harmonics without additional and complex magnetic interface [17]. However, as the number of levels increases, the incremental complexity exceeds the incremental benefits. For instance, to produce an output equivalent of a 48-pulse arrangement, an inverter with 31-levels is required [18].

Operating characteristics of STATCOM and UPFC are well established in the literature. However the SSSC has received little attention. Reference [6] discusses fundamental operating principles and performance characteristics of an SSSC and compares them to those characterizing the more conventional compensators based on TCSC or TSSC. The design, modeling, and control design of a 48 step SSSC is presented in [19-20]. In [21], a fuzzy logic based supplementary controller has been designed for SSSC to improve power system dynamic performance. A signal based on transmission line current has been used as a supplementary signal to the controller. In [22], a robust SSSC damping controller based on fuzzy logic has been designed for damping low frequency oscillations of power system. A PWM SSSC has been used to damp power system oscillations in [23]. But a systematic approach for design of damping controller and selection of operating point for designing damping controller for robust performance has not been presented. A PWM SSSC is considered in the present work. A systematic approach for designing damping controller using phase compensation method and selection of operating point for designing damping controller for robust performance are presented. The proposed procedure for designing SSSC based damping controller for robust performance is applied to a part of Indian power system.

1.3 Objectives and Scope of the Thesis

Our main interest is to design an SSSC based damping controller to damp the low frequency oscillations effectively over a wide range of operating conditions. The motivation for this study is the fact that unlike other FACTS controllers, SSSC has not received much attention. The objective and scope of the thesis are:

1. Systematic approach to design an SSSC based damping controller at nominal loading condition using phase compensation method and investigate the effectiveness of different controlling parameters.

7

2. Selection of operating point for designing an SSSC based damping controller to give robust performance over a wide range of operating conditions and variation in system parameters.

3. Application of the procedure adopted to design SSSC based damping controller to a part of Indian power system.

To achieve above objectives we use the IEEE model of single machine infinite bus system and practical system data is collected from POWER GRID CORPORATION OF INDIA LIMITED. We shall use the MATLAB simulink for simulation.

1.4 Outline of the Thesis

In Chapter 2, fundamental principles and characteristics of SSSC are presented. In this Chapter three-level PWM based SSSC is considered [15]. A brief review of this SSSC and its equivalent circuit models are presented. A power flow controller is designed for SSSC compensated power system. Simulation results using MATLAB simulink outlining the operation of SSSC are presented.

In Chapter 3, a systematic approach to design of SSSC based damping controller using phase compensation method is presented. The SSSC based damping controller is designed at nominal loading condition and effectiveness of different controlling parameters at wide range of operating conditions are investigated. Based on the results of simulation, selection of operating point for designing damping controller to give robust performance is presented. The performance of designed damping controllers are verified using eigen value analysis and simulation using MATLAB simulink. Performance of designed robust SSSC based damping controller under varying system parameter conditions was investigated.

In Chapter 4, procedure adopted in Chapter 3 is applied to a part of practical Indian transmission system to design damping controller to give robust performance at wide variation of loading and system parameters.

Chapter 5 summarizes the contribution of the present thesis and gives the scope for future research.

CHAPTER 2

PRINCIPLE, DESIGN AND MODELING OF
STATIC SYNCHRONOUS SERIES COMPENSATOR

Shunt compensation is ineffective in controlling actual transmitted power which, at a defined transmission voltage, is ultimately determined by the series line impedance and the angle between the ends of the line. It was always recognized that ac power transmission over long lines was primarily limited by the series reactive impedance. Series reactive compensation was introduced decades ago to cancel the portion of inductive reactance of transmission lines and thereby increase in transmittable power. Most of the presently used power flow controllers employ conventional thyristors in circuit arrangements, which are similar to breaker, switched capacitor and reactors, but have very fast response and are operated by sophisticated controls. All of these have common characteristics, in that the necessary reactive power required for the compensation are generated or absorbed by traditional capacitor or reactor banks, and thyristor switches are only used for controlling combined reactance offered by these banks during successive cycles of system voltage. Consequently thyristor controlled compensator presents variable reactive admittance to the system and therefore generally change the system impedance.

This chapter describes basic approach of series compensation for real time control of power flow in transmission line by using synchronous voltage source produced by voltage source converters. The concept of using the synchronous voltage source based on the fact that impedance verses frequency characteristics of the series capacitor, in contrast to filter application, plays no part in accomplishing the desired compensation of a transmission line. The function of the series capacitor is to produce voltage at fundamental frequency in quadrature with line current to compensate reactive voltage drop of transmission line, this will increase voltage across line thereby increase in transmittable power. Synchronous voltage source generated by three-level multi-bridge PWM converter. The work presented in this chapter is based on [15] namely "Performance analysis of SSSC based on three-level

multi-bridge PWM inverter". Simulation results of power flow controller for SSSC compensated power system are presented.

2.1 Fundamental Principles and Characteristics

The basic principles of SSSC can be explained with reference to the conventional series capacitive compensation of Fig 2.1 together with the related phasor diagram.
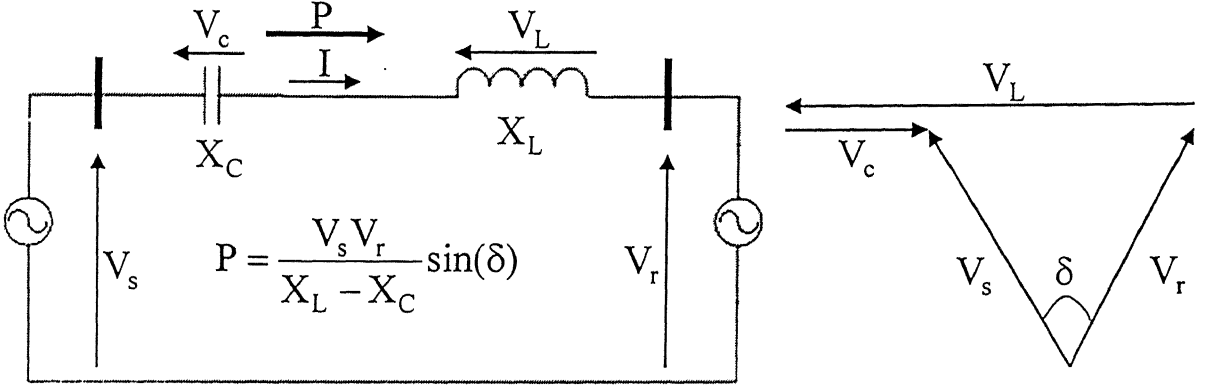
Fig 2.1 Basic two machine system with a series capacitor compensated transmission line and associated phasor diagram.

V_c is the injected compensating voltage phasor, I is the line current, X_c is the reactance of series capacitor, X_L is the line reactance, $k = X_c /X_L$ is the degree of series compensation. The phasor diagram clearly shows that at a given line current, voltage across the series capacitor forces opposite polarity voltage across line reactance to increase by the magnitude of the capacitor voltage, which is in phase opposition to reactive voltage drop across transmission line. Thus, the series compensation increases the voltage across the impedance of given transmission line, which increases the corresponding line current and transmittable power. While it may be convenient to consider series compensation is a means of reducing the line impedance but in reality it increases the voltage across impedance of transmission line. If the series compensation is provided by synchronous voltage source (SVS), as shown in Fig 2.2, output of SVS should precisely match the voltage of a series capacitor.

$$V_q = V_c = -jX_c.I = -jkX_L.I \qquad (2.1)$$

By making output voltage of SVS as function of line current, the same compensation, as provided by series capacitor, is accomplished. However unlike a series capacitor, SVS can produce output compensating voltage independent of magnitude of the line current. For normal capacitive compensation, the output voltage lags the line current by 90°. For SVS, the output voltage can be reversed by simple control action to make output voltage lead or lag the line current by 90°. If output voltage leads the line current by 90°, the compensating voltage decreases the voltage across impedance of the line and the series compensation has same effect as the line reactance was increased. The generalized expression for the injected voltage $\overline{V}_q$ is

$$\overline{V}_q = \pm j\, V_q(\zeta)\frac{\overline{I}}{I} \qquad\qquad (2.2)$$

$V_q(\zeta)$ is the magnitude of injected voltage and ζ is the chosen control parameter.

$$V_q = \pm j.V_q(\zeta).\frac{\overline{I}}{I}$$

$$P_q = \frac{V_s.V_r}{X_L - \dfrac{V_q}{I}}\sin\delta$$
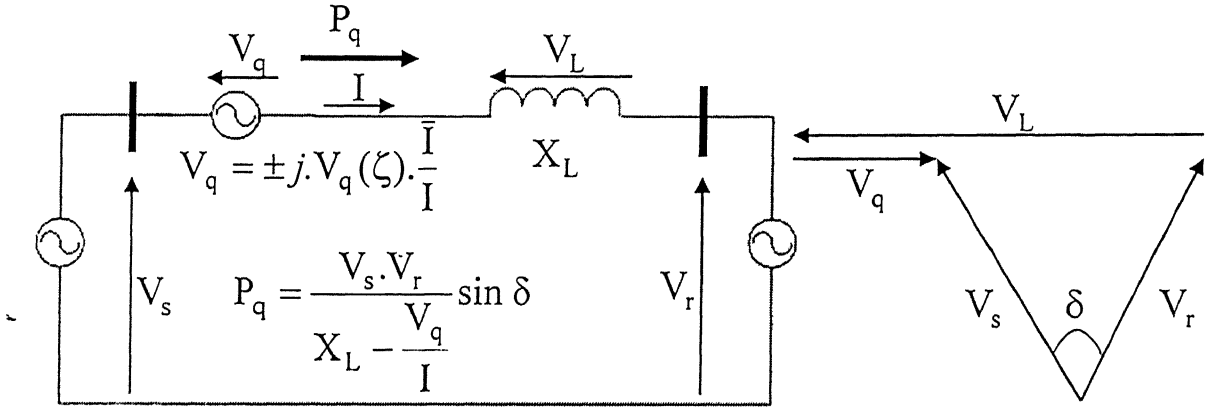
Fig 2.2 Basic two machine system with a SSSC compensated transmission line and associated phasor diagram

2.1.1 Transmitted power vs transmission angle characteristics

In fixed series capacitor compensation, the voltage across the capacitor is proportional to the line current, which is the function of the transmission angle. By changing the transmission angle, the line current will change. The transmitted power P can be expressed for two machine system as

$$P = \frac{V_s \cdot V_r}{X_L (1-k)} \operatorname{Sin}(\delta) \tag{2.3}$$

Where $V_s = V_1 \angle \delta_1$, $V_r = V_2 \angle \delta_2$, $\delta = \delta_1 - \delta_2$ and $k = \dfrac{X_c}{X_L}$ is the degree of series compensation.

Fig 2.3 shows the transmitted power verses transmission angle plots of series capacitor compensated two machine system for different values of k.

Note that for fixed series compensation, the power angle curve will be in the capacitive mode of operation. An SSSC can operate in both capacitive and inductive modes. Inductive mode of operation can be obtained by making the output voltage lead the line current by 90°.
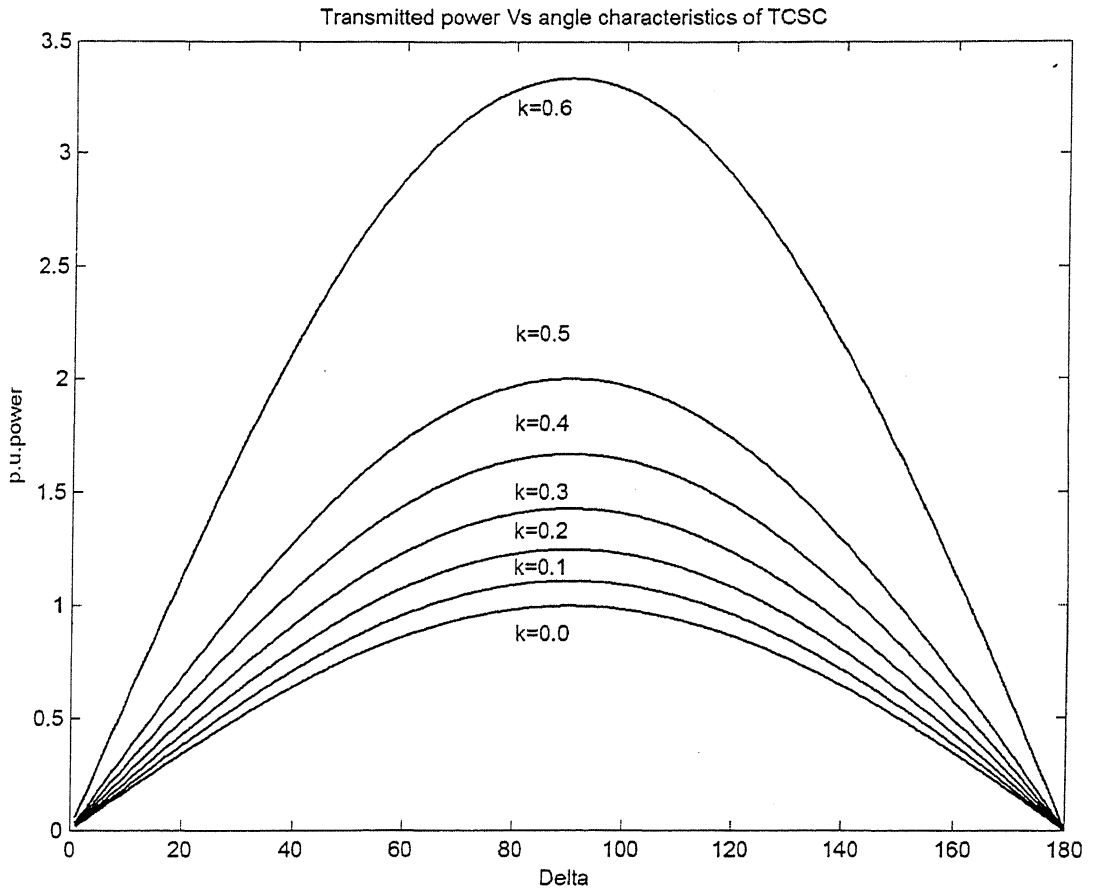
Fig 2.3 Transmitted power Vs transmission angle plots of two machine system compensated with series capacitor as a parametric function of degree of series compensation.

The power angle characteristics shown in Fig. 2.3 are same as that of characteristics of SSSC when it operates in capacitive regions, if the compensating voltage is injected in series with line. The compensating voltage is in proportional to the line current.

If the SSSC injects compensating voltage in series with the line irrespective of the magnitude of line current, the transmitted power versus angle relationship becomes parametric function the injected voltage (V_q). The transmitted power P_q can be expressed for a two machine system as:

$$P_q = \frac{V_s V_r}{X} \sin(\delta) + \frac{V_s}{X} V_q \cos\left(\frac{\delta}{2}\right)$$

(2.4)

The normalized power angle characteristics as a parametric function V_q are shown in Fig 2.4 for $V_q = 0, \pm 0.353, \pm 0.707$.
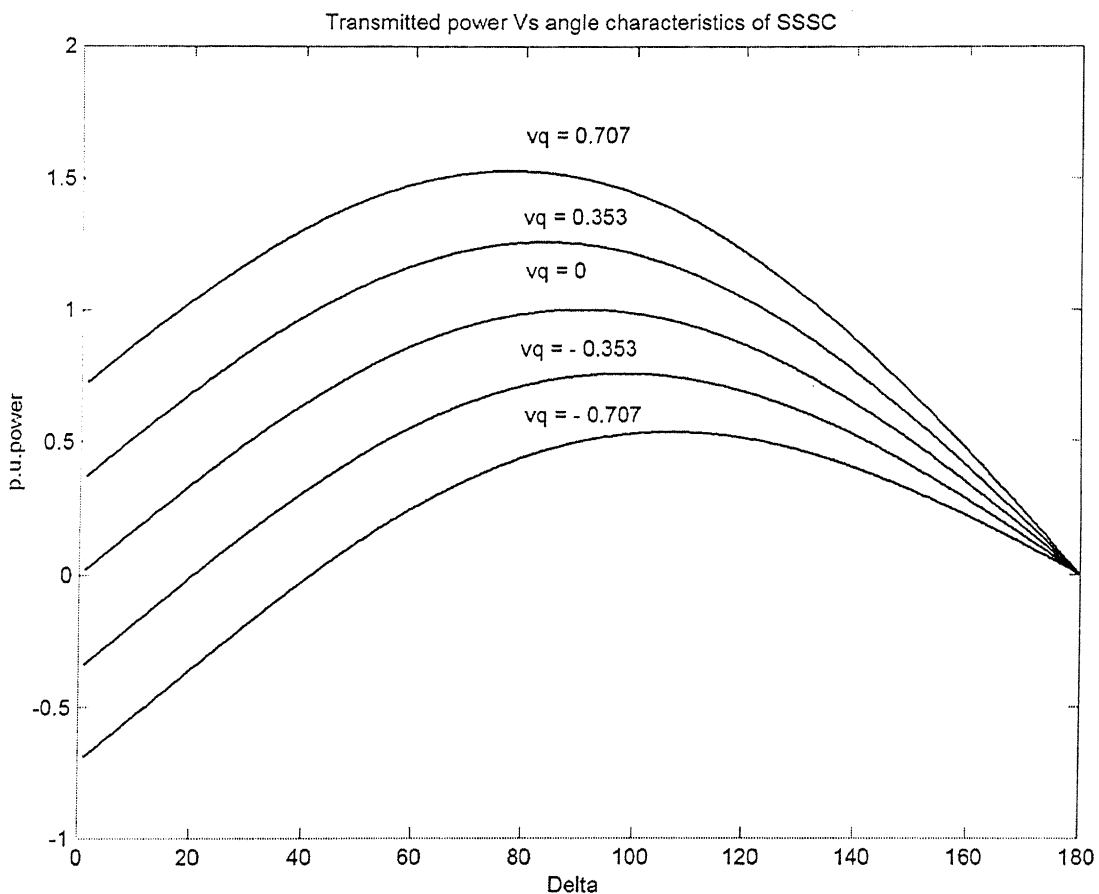
Fig 2.4 Transmitted power Vs transmission angle plots of two machine system compensated with SSSC as a parametric function of magnitude of series compensating voltage.

Comparing plots in Fig 2.3 and 2.4, it can be seen that series capacitor increases the transmitted power by a fixed percentage of power transmitted by the uncompensated line at a given δ. On the other hand, SSSC increases the transmitted power by a fixed percentage of power transmitted by uncompensated line independent of δ. An additional difference evident in these plots is that the capacitor can only increase the transmittable power, the SSSC can also decrease it, simply by reversing the injected voltage. The reversed voltage adds directly to the reactive voltage drop of line as if the reactance of line increased.

2.1.2 Comparison of SSSC with TCSC

SSSC is the voltage source type compensator where as TCSC is the variable impedance type compensator. The voltage source type of SSSC offers some inherent capabilities and functional features for series line compensation which may not be attainable with variable impedance type compensators. These characteristics and features of SSSC and TCSC are summarized as follows [6, 10].

1. The SSSC is capable of internally generating a controllable compensating voltage over an identical capacitive and inductive range independent of the magnitude of line current. The TCSC can maintain maximum compensating voltage with decreasing line current over a control range determined by the current boosting capability of thyristor controlled reactor.

2. The SSSC has inherent ability to interface with an external dc power supply to provide compensation for the line resistance by injection of real power, as well as line reactance by injection of reactive power. TCSC can't exchange real power with the transmission line and can only provide reactive compensation.

3. The SSSC with energy storage increases the effectiveness of power oscillation damping by modulating the series reactive compensation to increase or decrease the transmitted power, and by concurrently injecting an alternating virtual positive and negative real impedance to absorb and supply real power from line in sympathy with the prevalent machine swings. The TCSC can damp the oscillations only by modulated reactive compensation affecting the transmitted power.

4. TCSCs are coupled directly to the line and therefore are installed on a high voltage platform. The cooling system and control are located on the ground with high voltage insulation requirements and control interface. The SSSC requires a coupling transformer, and it is installed in a building at ground potential and operated at relatively low voltage.

5. TCSC employs conventional thyristors, these are available with the highest current and voltage ratings, and they also have highest surge current capability. SSSC uses GTO thyristors. These devices presently have lower voltage and current ratings, and considerably lower short term surge current rating.

In addition, TCSC suffers from some other disadvantages. It injects low order harmonics (typically 3rd, 5th, 7th) into power system because of thyristor phase control. Transient response of circuit is rather slow, because of control of firing pulse is available only once in each half cycle. TCSC is susceptible to parallel resonance due to presence of inductor and capacitor in parallel paths.

2.2 Synchronous Voltage Source

The switching power converters can have capability of generating controlled reactive power directly without the use of capacitor or reactor. These converters are operated as voltage or current sources and produce reactive power essentially without reactive energy storage components by circulating alternating current among the phases of the ac system. Functionally, from the stand point of reactive power generation, their operation is similar to that of an ideal synchronous machine whose reactive output is varied by excitation control. They can also exchange real power with ac system if supplied from appropriate dc energy source [13]. Because of these similarities with rotating synchronous generators, they are termed as static synchronous voltage generators or static synchronous voltage source.

Converters presently employed for FACTS controller are voltage source converters (VSC), because of VSC having following advantages over current source converter (CSC).

1. Current source converters require power semiconductors with bi-directional voltage blocking capability. The available high power semiconductors with gate turn off capability either can't block reverse voltage at all or can do it with increased losses.

2. Practical current source termination of the converter dc terminals by a current charged reactor is much lossier than complementary voltage source termination by a voltage charged capacitor.

3. The current source converter requires a voltage source termination at ac terminals, usually in the form of a capacitive filter. The voltage-sourced converter requires a current termination at the ac terminals that is naturally provided by leakage impedance of coupling transformer.

The maximum sustain voltage of the currently available GTO for FACTS application is about 5 kV, which is far less than the operation voltage of power system. To solve this problem, step down transformers are used for properly interfacing facts devices with the power system, and the power converters with series connected GTO's are used. Although series connection of GTO's is a proven technology, there is still restriction in maximum allowable number of units. Multi-level inverter was considered to increase the system operating voltage avoiding series connection of switching devices. However multi-level inverter has complexity in the formation of output voltage and requires many back connection diodes. In order to complement this multi-bridge inverter, with pulse amplitude modulation [15], 6 H-bridge modules per phase was used.

2.2.1 Three-level multi-bridge PWM inverter

The VSC in Fig 2.5 consists of six three-level half bridge modules per phase. The principle of operation of one module can be explained using ideal switch GTO and back to back connected diode.

The output of each module has three states $+V_{dc}/2$, 0, $-V_{dc}/2$, depending on the state of inverter switches S1-S4. Table 1 shows relation between output voltage and switching state. By adjusting time duration of conduction output voltage can be adjusted.

Table 1: Switching pattern of three level half bridge

Voltage	Switching state
$V_{dc}/2$	S1,S2: on and S3, S4: off
0	S2,S3: on and S1, S4: off
0	S1,S4: on and S2, S3: off
$-V_{dc}/2$	S3,S4: on and S1, S2: off
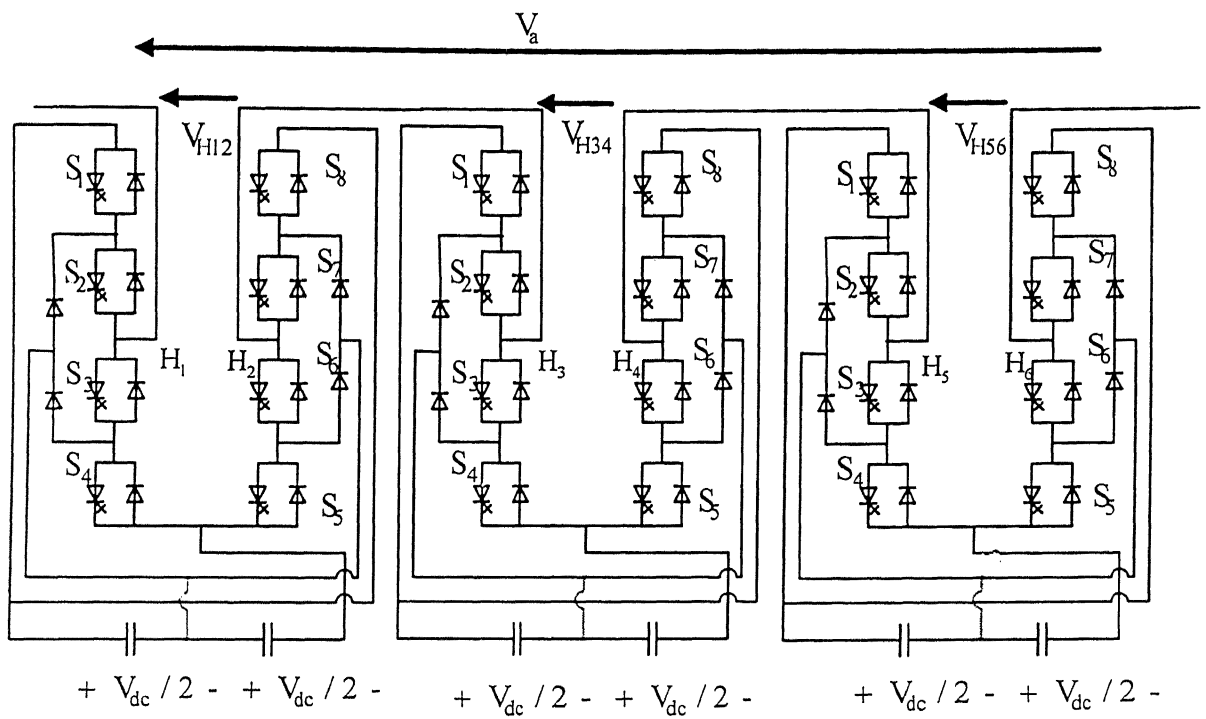
Fig 2.5 Three-level multi-bridge inverter with pulse width modulation (PWM)
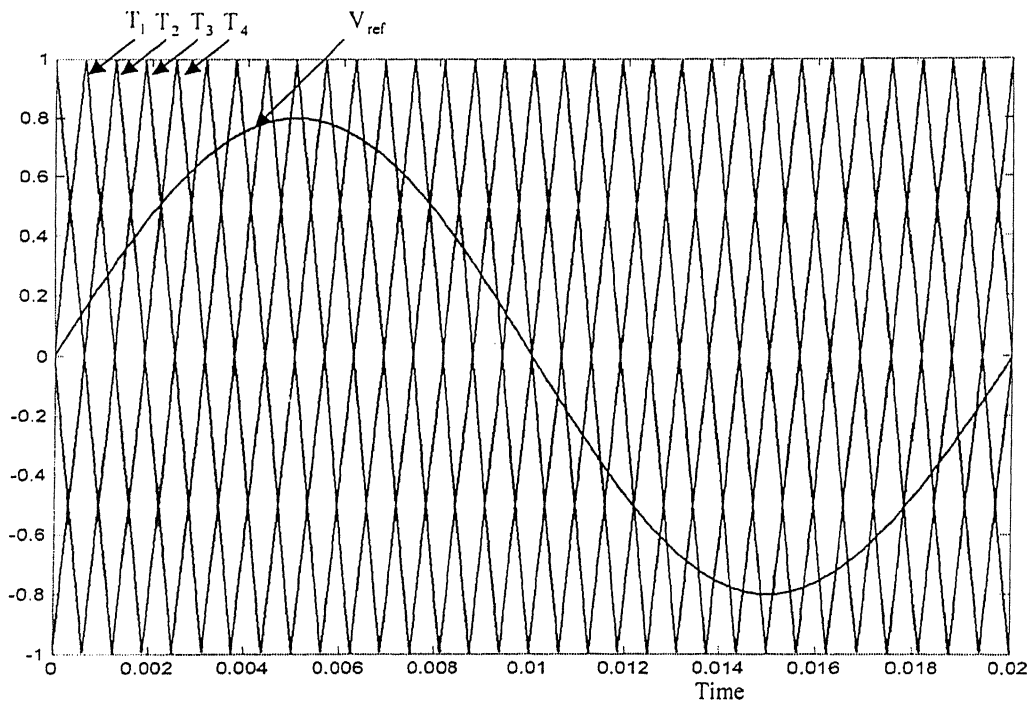
Fig.2.6 Carrier and reference signal

17
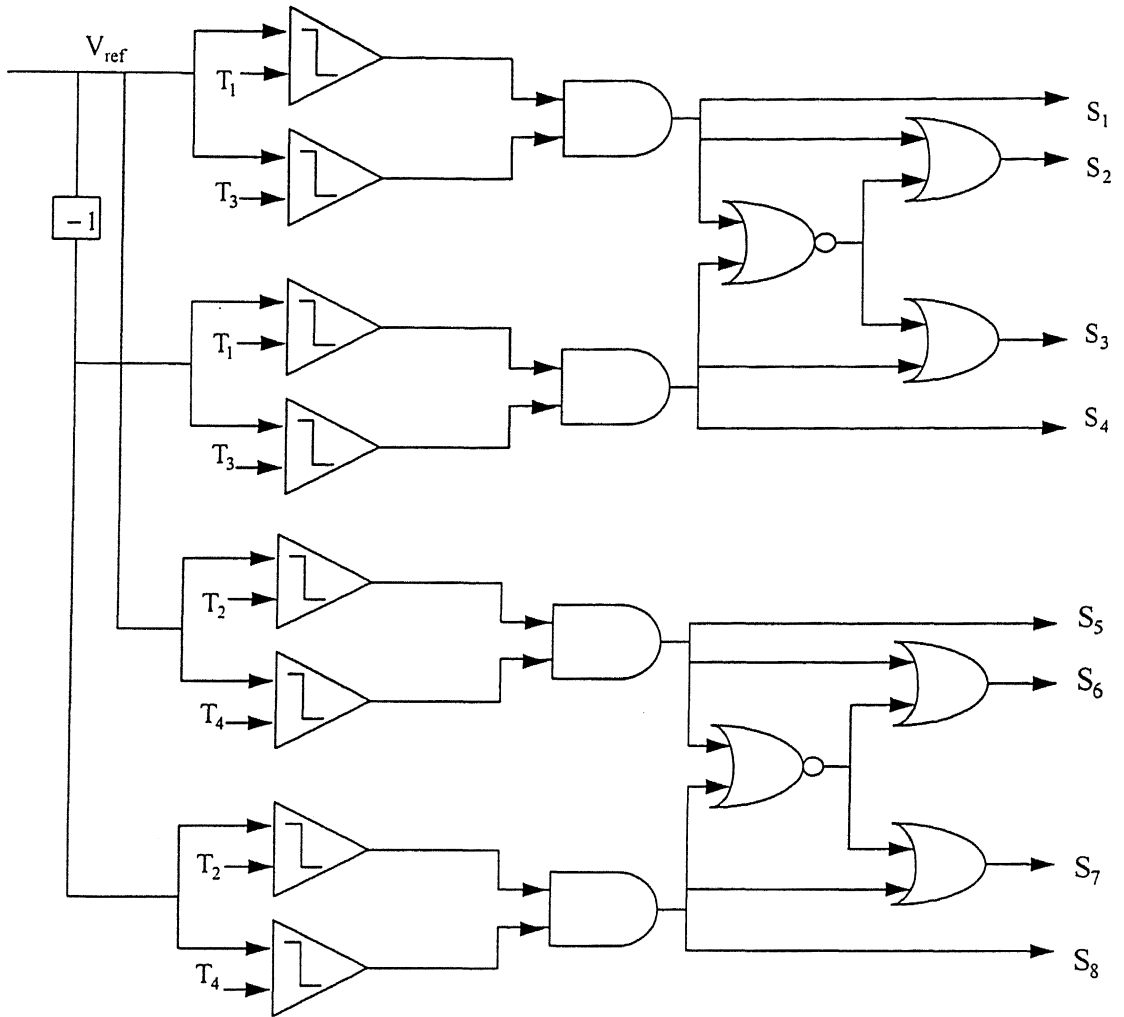
Fig. 2.7 Gate pulse generation scheme

Fig 2.5 shows three-level multi-bridge inverter with pulse width modulation (PWM) scheme. Fig. 2.6 shows four carrier and one reference signal to generate gate pulses for inverter module H1, H2. The frequency of carrier T1, T2, T3, T4 is 400 Hz. Each of Four carriers has 90° phase shift with each other. The reference signal V_{ref} has sinusoidal wave form of 50Hz. Fig. 2.7 shows generation of gate pulses using reference and carrier. Carrier T1 and T3 used to generate the gate pulses for module H1. The gate pulses for module H2 can be obtained by using same procedures as that for module H1 except that carrier T1&T3 is replaced with T2 and T4. Two sets of four are carriers required to generate gate pulses for building up output voltage of H34 and H56 inverter group. These sets of carrier have 120°

18

phase shift with each other. Fig. 2.8 shows the output voltage of each inverter group H12, H34, H56. Fig. 2.9 shows the total output voltage V_A ($V_{H12}+V_{H34}+V_{H56}$) of three inverter groups. FFT analysis result is shown in Fig. 2.10. THD of the output voltage is around 8% and spectra of harmonics are located around 5 kHz. Since each carrier has 400 Hz and there are 12 carriers, total output voltage has an equivalent switching effect of 4.8 kHz. Therefore these harmonics can be easily filtered out.
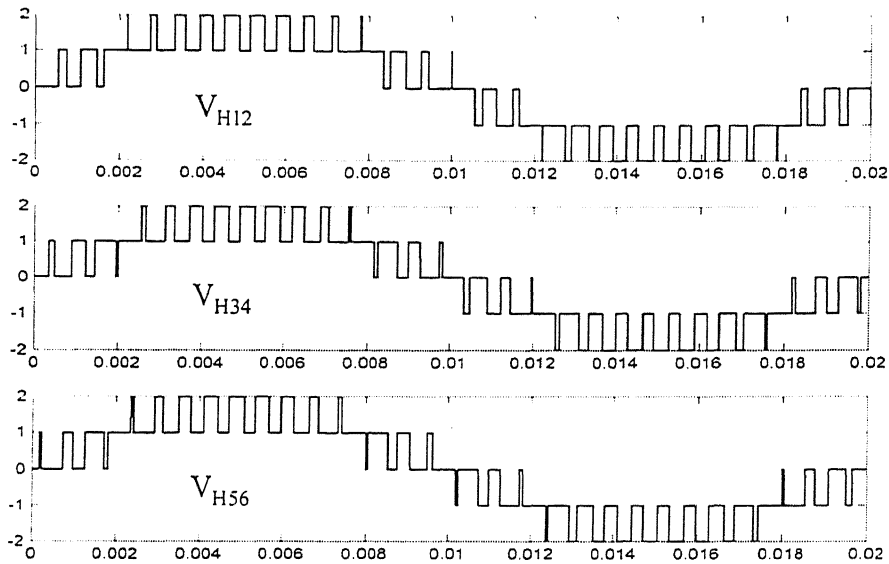
Fig. 2.8 output voltage of inverter groups H_{12}, H_{34}, H_{56}.
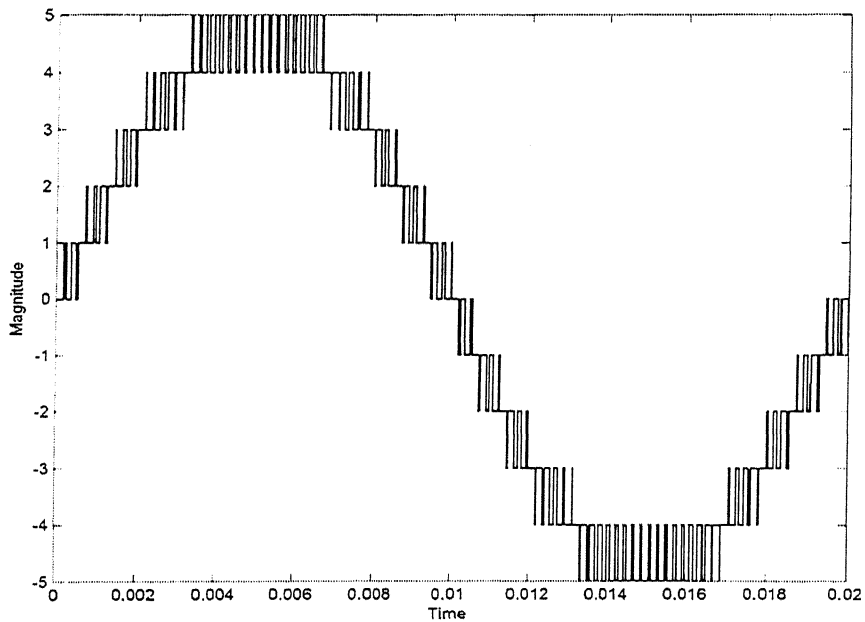
Fig.2.9 Output voltage of Three level multi bridge PWM inverter
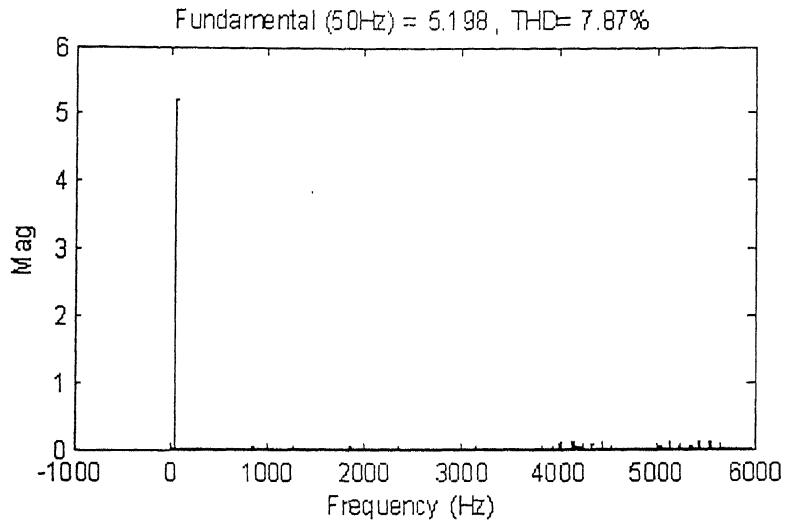
Fig. 2.10 Fourier analysis of output voltage of inverter.

2.3 Modeling of SSSC
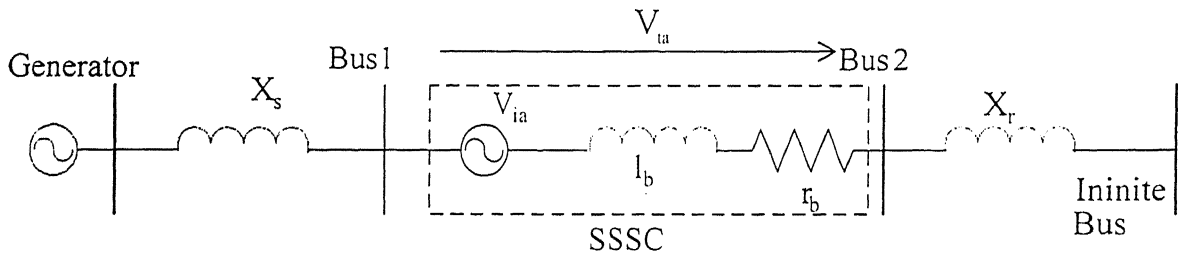
Fig. 2.11 Single line diagram of SSSC compensated power system

The equivalent circuit of Multi-level PWM inverter is connected in series with transmission line as shown in Fig. 2.11. The dynamic equation of three-level multi-bridge PWM inverter based SSSC can be written as

$$V_{ta} = V_{ia} + R_r i_a + l_b \frac{di_a}{dt}$$
(2.5)

V_{ia} is inverter output voltage of phase –a

V_{ta} is voltage of phase-a between bus 1 & 2.

i_a is the phase-a current of transmission line

Similar equations can be written for other two phases also. The overall equations including dc side given are given by [24]

Similar equations can be written for other two phases also. The overall equations including dc side given are given by [24]

$$\begin{bmatrix} \dfrac{di_a}{dt} \\[2mm] \dfrac{di_b}{dt} \\[2mm] \dfrac{di_c}{dt} \end{bmatrix} = \begin{bmatrix} -\dfrac{r_b}{l_b} & 0 & 0 \\[2mm] 0 & -\dfrac{r_b}{l_b} & 0 \\[2mm] 0 & 0 & -\dfrac{r_b}{l_b} \end{bmatrix} \begin{bmatrix} i_a \\ i_b \\ i_c \end{bmatrix} - \dfrac{mk\sigma V_{dc}}{2l_b} \begin{bmatrix} \cos(\omega t + \delta_b) \\ \cos(\omega t + \delta_b - 120) \\ \cos(\omega t + \delta_b + 120) \end{bmatrix} + \begin{bmatrix} \dfrac{1}{l_b} & 0 & 0 \\[2mm] 0 & \dfrac{1}{l_b} & 0 \\[2mm] 0 & 0 & \dfrac{1}{l_b} \end{bmatrix} \begin{bmatrix} V_a \\ V_b \\ V_c \end{bmatrix} \quad (2.6)$$

$$\frac{dV_{dc}}{dt} = \frac{mk\sigma}{2C_{dc}}\begin{bmatrix} \cos(\omega t + \delta_b) & \cos(\omega t + \delta_b - 120) & \cos(\omega t + \delta_b + 120) \end{bmatrix}\begin{bmatrix} i_a \\ i_b \\ i_c \end{bmatrix} \quad (2.7)$$

m is the amplitude modulation index of inverter, δ_b is the phase angle of inverter output voltage, σ is the transformation ratio of coupling transformer, k is the no. of H bridges per phase.

Converting the above equations in d-q frame and normalising in p.u, we get

$$\begin{bmatrix} \dfrac{di_d}{dt} \\[2mm] \dfrac{di_q}{dt} \\[2mm] \dfrac{di_0}{dt} \end{bmatrix} = \begin{bmatrix} 0 & \omega & 0 \\ -\omega & 0 & 0 \\ 0 & 0 & 0 \end{bmatrix}\begin{bmatrix} i_d \\ i_q \\ i_0 \end{bmatrix} + \begin{bmatrix} -\dfrac{r_b}{l_b} & 0 & 0 \\[2mm] 0 & -\dfrac{r_b}{l_b} & 0 \\[2mm] 0 & 0 & -\dfrac{r_b}{l_b} \end{bmatrix}\begin{bmatrix} i_d \\ i_q \\ i_0 \end{bmatrix} - \dfrac{mk\sigma V_{dc}}{2l_b}\begin{bmatrix} \cos\delta_b \\ \sin\delta_b \\ 0 \end{bmatrix} + \begin{bmatrix} \dfrac{1}{l_b} & 0 & 0 \\[2mm] 0 & \dfrac{1}{l_b} & 0 \\[2mm] 0 & 0 & \dfrac{1}{l_b} \end{bmatrix}\begin{bmatrix} V_d \\ V_q \\ V_0 \end{bmatrix}$$

$$(2.8)$$

$$\frac{dV_{dc}}{dt} = \frac{3mk\sigma}{4C_{dc}}\begin{bmatrix} \cos\delta_b & \sin\delta_b & 0 \end{bmatrix}\begin{bmatrix} i_d \\ i_q \\ i_0 \end{bmatrix} \quad (2.9)$$

Suffixes d, q indicates the equivalents of the corresponding three phase quantities in the transformed system.

2.4 Power Flow Control Using SSSC

Fig. 2.11 shows an SSSC connected in series with a simple transmission line between Bus1 and Bus2. The transmission line has an inductive reactance X_s, and a voltage source V_s at the sending end and inductive reactance X_r, and a voltage source V_r at receiving end respectively. Fig. 2.12 shows control block diagram of SSSC. An instantaneous set of line voltages, v_1, at Bus 1 is used to calculate the reference angle, θ, which is phase locked to the

phase-a of the line voltage v_{la}. An instantaneous three-phase set of measured line current I, is first decomposed into its real component i_d, and reactive component, i_q. Then the amplitude I and the relative angle, θ_{ir}, of the current with respect to the phase locked angle θ, are calculated. The phase angle, θ_i, of the line current calculated by adding the relative angle, θ_{ir} of the line current and phase locked angle, θ. The calculated amplitude, I of the line current multiplied by the corresponding line reactance demand, X_q^*, is the injected voltage amplitude demand, v_q^*. The phase angle θ_{ref} of the injected voltage demand is θ_i+90, if the demanded compensation is inductive or θ_i-90, if the demanded compensation is capacitive. The dc link voltage is dynamically regulated in relation with the insertion voltage amplitude demand. The insertion voltage amplitude demand v_q^*, and the dc link voltage demand v_{dc}^*, are related to inverter DC to fundamental ac amplitude gain factor. The dc link capacitor voltage demand v_{dc}^*, and the measured dc link capacitor voltage are compared and the error is passed through an error amplifier (PI controller) which produces angle β. The phase angle, δ_b, of the inverter voltage is calculated by adding angle, β and the angle of inserted voltage demand θ_{ref}. The compensating reactance demand X_q^*, is either negative if the SSSC is emulating an inductive reactance or positive if it is emulating capacitive reactance. In some other applications, the insertion voltage demand is directly specified and the SSSC injects the desired voltage almost in quadrature with line current.
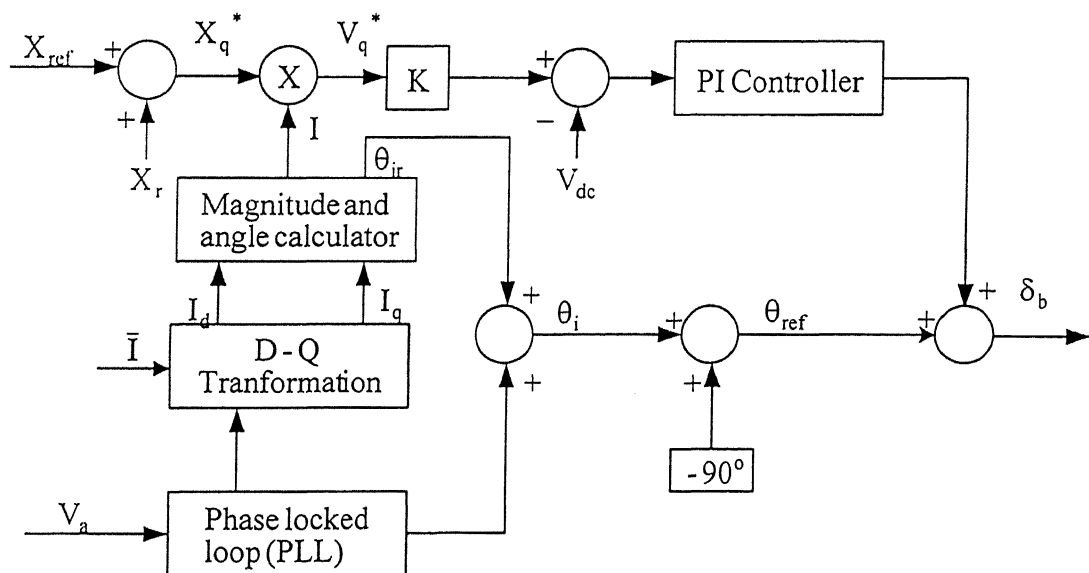
Fig.2.12 Control block diagram of SSSC

The purpose of PI controller is to maintain the charge on the dc capacitor and to inject a voltage in quadrature with the line current. If the injected voltage is not in quadrature with line current, real power exists at the ac terminals of the inverter, which then either charges or discharges the dc capacitor, resulting in deviation of dc capacitor voltage from set point. The PI controller then advances or retards the phase of the injected voltage relative to the line current in order to adjust power at ac terminals and keep the dc voltage constant. At steady state, when the dc voltage remains constant, no real power is exchanged at the ac terminals.

2.5 Simulation Results

The feasibility of power flow controller is demonstrated by simulation of three-level multi-bridge PWM based SSSC power flow controller using MATLAB Simulink package. The system used for simulation is given in Appendix-I, while simulation the generator and infinite bus are replaced by equivalent voltage sources. The receiving end voltage lag the sending voltage by an angle 30°. The value of DC capacitor chosen to be 2000μF. Fig 2.13 shows simulation results when SSSC emulates capacitor in series with transmission line. The SSSC is connected to the uncompensated line at 3 sec. with a capacitive reactive demand of 0.2 p.u. When the SSSC is connected to system, the line current and power flow in the system increases. At 6 sec. the compensation increases to 0.3 p.u and there is the corresponding increase in line current, power, dc voltage and injected voltage. At 9 sec. the compensation reduced to 0.1 p.u to decrease the power flow. The amplitude of injected voltage is proportional to dc link voltage. The Fig 2.14 shows the inverted output voltage and line current when the compensation level is 0.3 p.u, it shows phase angle between these quantities is 90°.
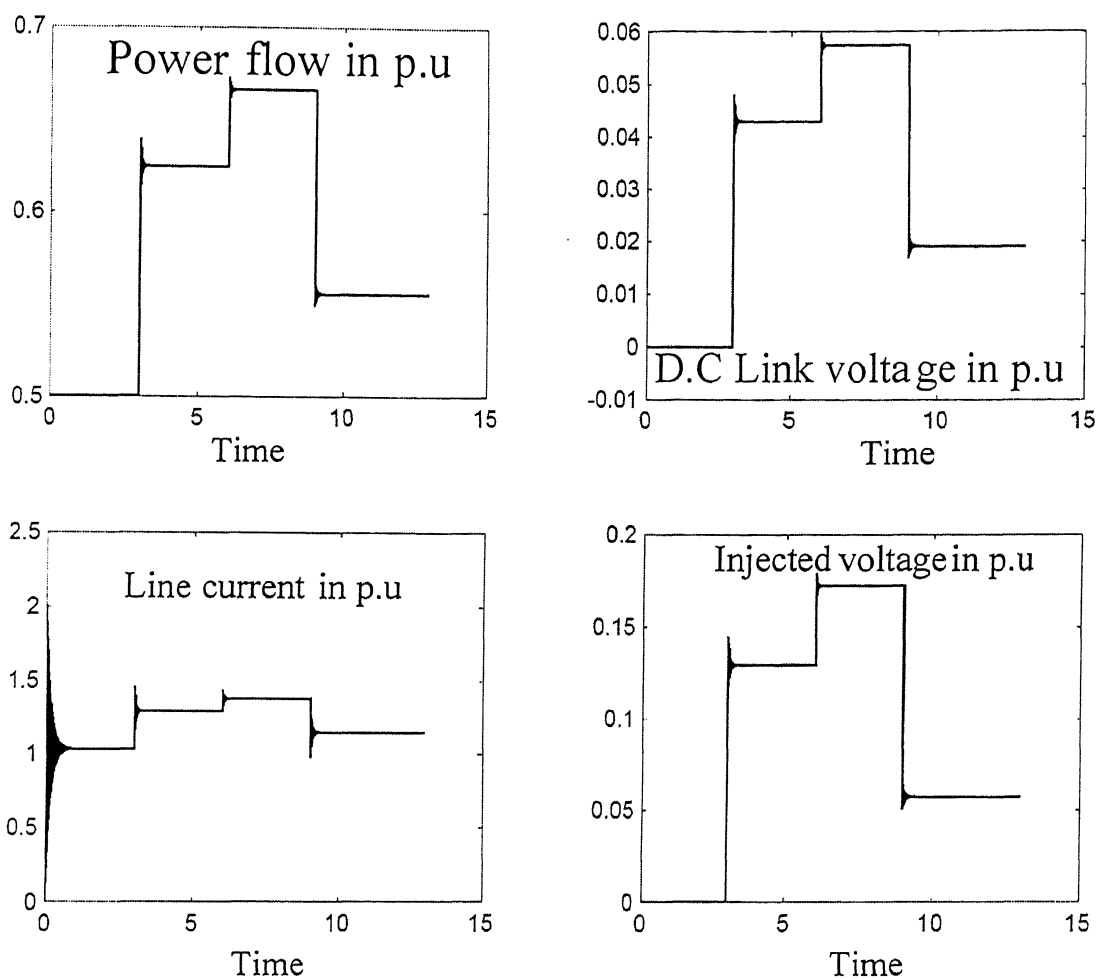
Fig. 2.13 Simulation results of SSSC power flow controller
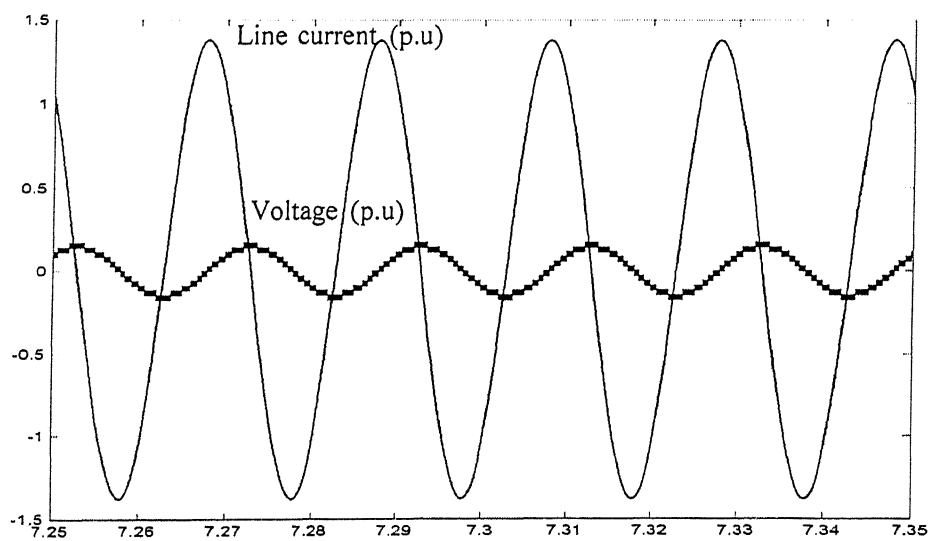
Fig 2.14 Phase relation between SSSC injected voltage and line current

2.6 Conclusions

Fundamental principles, design and modeling of SSSC are given in this Chapter. In contrast to the fixed capacitor, the SSSC maintains a constant compensating voltage in the presence of variable line current, or control the amplitude of injected voltage independent of amplitude of line current. Three-level multi-bridge pulse width modulation technique has been used for implementing synchronous voltage source of SSSC. Three level multi bridge PWM based SSSC power flow control by adjusting dc capacitor voltage has been demonstrated by simulation.

CHAPTER 3

DESIGN AND SIMULATION OF DAMPING CONTROLLER USING PHASE COMPENSATION METHOD

Low frequency oscillations are very harmful for power systems, especially in the deregulated electric utility industry where steady increase in long-distance power transfers makes the situation grave. Conventional methods, such as Power System Stabilizers (PSSs), however, may not be so effective to deal with various oscillation modes emerging in large scale, complex and deregulated electricity industries. To damp out the low frequency oscillations, an SSSC based damping controller using phase compensation method is proposed and a systematic approach for designing the damping controller and the selection of robust operating condition for the design of the damping controller has been attempted.

3.1 SSSC Compensated Power System Model
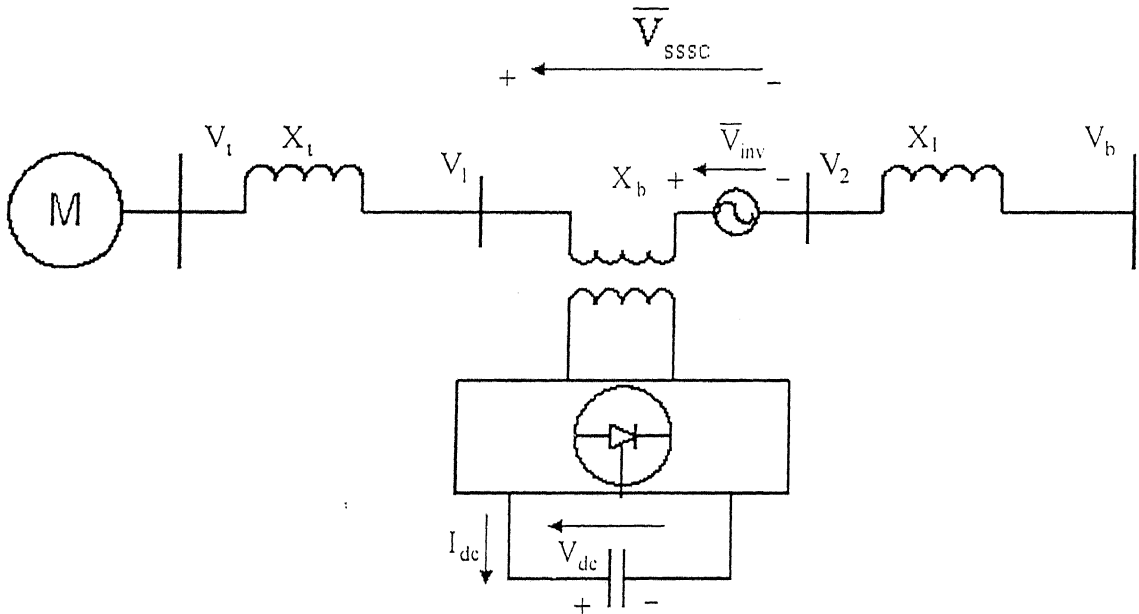
Fig. 3.1 Single machine infinite bus power system with a SSSC

26
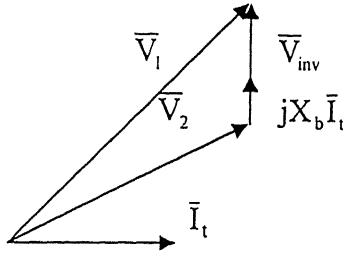
Fig. 3.2 (a). SSSC in inductive mode   (b). SSSC in capacitive mode
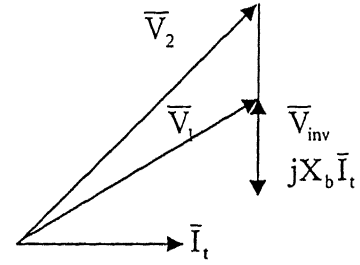
A single machine infinite bus power system installed with a SSSC is shown in Fig 3.1. This consists of a series coupling transformer (SCT) with a leakage reactance Xsct, a three phase GTO based voltage converter (VSC) and a DC capacitor. The exchange of reactive power between SSSC and power system is achieved by controlling the magnitude and phase of the inserted voltage which is kept in quadrature with the line current.

Fig 3.2 shows the phasor diagrams for SSSC operation, from which we can see that the compensation level can be controlled dynamically by changing the magnitude of inverter output voltage $\overline{V}_{inv}$. Hence SSSC is expected to be effective in damping out power system oscillations if it is equipped with a damping controller. If pulse width modulation (PWM) wave form synthesis is used, PWM amplitude modulation index (m) or phase angle of the inverter output voltage (δ) can be the damping control signal to provide the dynamic compensation.

Dynamic equations of the synchronous machine are given as fallows

$$\dot{\delta} = \omega_b \omega$$

$$\dot{\omega} = (P_m - P_e - D\omega)/M$$

$$\dot{E}'_q = (-E_q + E_{fd})/T'_{do}$$

$$\dot{E}_{fd} = -\frac{1}{T_A}E_{fd} + \frac{K_A}{T_A}(V_{to} - V_t)$$

(3.1)

where

$$P_e = E'_q I_q + (x_q - x'_d)I_d I_q$$

$$E_q = E'_q + (x_d - x'_d)I_d$$

$$V_t = \sqrt{(E'_q - x'_d I_d)^2 + (x_q I_q)^2}$$

27

Dynamic Equations of SSSC

$$\begin{bmatrix} \dfrac{di_a}{dt} \\[2mm] \dfrac{di_b}{dt} \\[2mm] \dfrac{di_c}{dt} \end{bmatrix} = \begin{bmatrix} -\dfrac{r_b}{l_b} & 0 & 0 \\[2mm] 0 & -\dfrac{r_b}{l_b} & 0 \\[2mm] 0 & 0 & -\dfrac{r_b}{l_b} \end{bmatrix} \begin{bmatrix} i_a \\ i_b \\ i_c \end{bmatrix} - \dfrac{mk\sigma V_{dc}}{2l_b} \begin{bmatrix} \cos(\omega t + \delta_b) \\ \cos(\omega t + \delta_b - 120) \\ \cos(\omega t + \delta_b + 120) \end{bmatrix} + \begin{bmatrix} \dfrac{1}{l_b} & 0 & 0 \\[2mm] 0 & \dfrac{1}{l_b} & 0 \\[2mm] 0 & 0 & \dfrac{1}{l_b} \end{bmatrix} \begin{bmatrix} V_a \\ V_b \\ V_c \end{bmatrix} \tag{3.2}$$

$$\dfrac{dV_{dc}}{dt} = \dfrac{mk\sigma}{2C_{dc}} \begin{bmatrix} \cos(\omega t + \delta) & \cos(\omega t + \delta - 120) & \cos(\omega t + \delta + 120) \end{bmatrix} \begin{bmatrix} i_a \\ i_b \\ i_c \end{bmatrix} \tag{3.3}$$

By applying Park's transformation

$$P\begin{bmatrix} \dfrac{di_a}{dt} \\[2mm] \dfrac{di_b}{dt} \\[2mm] \dfrac{di_c}{dt} \end{bmatrix} = P\begin{bmatrix} -\dfrac{r_b}{l_b} & 0 & 0 \\[2mm] 0 & -\dfrac{r_b}{l_b} & 0 \\[2mm] 0 & 0 & -\dfrac{r_b}{l_b} \end{bmatrix} P^{-1}P\begin{bmatrix} i_a \\ i_b \\ i_c \end{bmatrix} - \dfrac{mk\sigma V_{dc}}{2l_b} P\begin{bmatrix} \cos(\omega t + \delta_b) \\ \cos(\omega t + \delta_b - 120) \\ \cos(\omega t + \delta_b + 120) \end{bmatrix} + P\begin{bmatrix} \dfrac{1}{l_b} & 0 & 0 \\[2mm] 0 & \dfrac{1}{l_b} & 0 \\[2mm] 0 & 0 & \dfrac{1}{l_b} \end{bmatrix} P^{-1}P\begin{bmatrix} V_a \\ V_b \\ V_c \end{bmatrix} \tag{3.4}$$

$$P\dfrac{dV_{dc}}{dt} = P\dfrac{mk\sigma}{2C_{dc}} \begin{bmatrix} \cos(\omega t + \delta) & \cos(\omega t + \delta - 120) & \cos(\omega t + \delta + 120) \end{bmatrix} P^{-1}P\begin{bmatrix} i_a \\ i_b \\ i_c \end{bmatrix} \tag{3.5}$$

where

$$P = \dfrac{2}{3}\begin{bmatrix} \cos\omega t & \cos(\omega t - 120) & \cos(\omega t + 120) \\ -\sin\omega t & -\sin(\omega t - 120) & -\sin(\omega t + 120) \\ 0.5 & 0.5 & 0.5 \end{bmatrix}$$

By substituting P in the above equations we can obtain

$$\begin{bmatrix} \dfrac{di_d}{dt} \\[2mm] \dfrac{di_q}{dt} \\[2mm] \dfrac{di_0}{dt} \end{bmatrix} = \begin{bmatrix} 0 & \omega & 0 \\ -\omega & 0 & 0 \\ 0 & 0 & 0 \end{bmatrix}\begin{bmatrix} i_d \\ i_q \\ i_0 \end{bmatrix} + \begin{bmatrix} -\dfrac{r_b}{l_b} & 0 & 0 \\[2mm] 0 & -\dfrac{r_b}{l_b} & 0 \\[2mm] 0 & 0 & -\dfrac{r_b}{l_b} \end{bmatrix}\begin{bmatrix} i_d \\ i_q \\ i_0 \end{bmatrix} - \dfrac{mk\sigma V_{dc}}{2l_b}\begin{bmatrix} \cos\delta_b \\ \sin\delta_b \\ 0 \end{bmatrix} + \begin{bmatrix} \dfrac{1}{l_b} & 0 & 0 \\[2mm] 0 & \dfrac{1}{l_b} & 0 \\[2mm] 0 & 0 & \dfrac{1}{l_b} \end{bmatrix}\begin{bmatrix} V_d \\ V_q \\ V_0 \end{bmatrix} \tag{3.6}$$

$$\dfrac{dV_{dc}}{dt} = \dfrac{3mk\sigma}{4C_{dc}}\begin{bmatrix} \cos\delta_b & \sin\delta_b & 0 \end{bmatrix}\begin{bmatrix} i_d \\ i_q \\ i_0 \end{bmatrix} \tag{3.7}$$

28

$$\frac{dV_{dc}}{dt} = \frac{3mk\sigma}{4C_{dc}} \begin{bmatrix} \cos\delta_b & \sin\delta_b & 0 \end{bmatrix} \begin{bmatrix} i_d \\ i_q \\ i_0 \end{bmatrix} \tag{3.7}$$

For the study of the power system oscillation stability, we can ignore the resistance and transients of the transformer of SSSC, then the above equations become

$$\begin{bmatrix} V_d \\ V_q \end{bmatrix} = \begin{bmatrix} 0 & -X_b \\ X_b & 0 \end{bmatrix} \begin{bmatrix} i_d \\ i_q \end{bmatrix} + \begin{bmatrix} \dfrac{mk\sigma V_{dc}\cos\delta_b}{2} \\ \dfrac{mk\sigma V_{dc}\sin\delta_b}{2} \end{bmatrix} \tag{3.8}$$

$$\frac{dV_{dc}}{dt} = \frac{3mk\sigma}{4C_{dc}} \begin{bmatrix} \cos\delta_b & \sin\delta_b \end{bmatrix} \begin{bmatrix} i_d \\ i_q \end{bmatrix} \tag{3.9}$$

From the network of Single machine infinite bus with SSSC (Fig 3.1)

$$V_t - \bar{I}.j(x + x_b) = \overline{V} + V_b \tag{3.10}$$

By representing above equation on the d-q co ordinates

$$x_q i_q + j(E'_q - x'_d i_d) - j(x + x_b)\bar{I} = \overline{V} + V_b \sin\delta + jV_b \cos\delta \tag{3.11}$$

Output voltage of the PWM inverter

$$\overline{V} = mk\sigma V_{dc}(\cos\delta_b + j\sin\delta_b) \tag{3.12}$$

$$= mk\sigma V_{dc}\angle\delta_b$$

$$\frac{dV_{dc}}{dt} = \frac{mk\sigma}{C_{dc}}(I_d \cos\delta_b + I_q \sin\delta_b) \tag{3.13}$$

$$I_q = \frac{V_b \sin\delta + mk\sigma V_{dc}\cos\delta_b}{x + x_b + x_q} \tag{3.14}$$

$$I_d = \frac{E'_q - V_b \cos\delta - mk\sigma V_{dc}\sin\delta_b}{x + x_b + x'_d} \tag{3.15}$$

$$\Delta\dot{\delta} = \omega_b \Delta\omega \tag{3.16}$$

$$\Delta\dot{\omega} = \left(-\Delta P_e - D\Delta\omega\right)/M$$

$$\Delta\dot{E}'_q = \left(-\Delta E_q + \Delta E_{fd}\right)/T'_{do} \tag{3.17}$$

$$\Delta\dot{E}_{fd} = -\frac{1}{T_A}\Delta E_{fd} + \frac{K_A}{T_A}\left(-\Delta V_t\right) \tag{3.18}$$

$$\tag{3.19}$$

$$\dot{V}_{dc} = K_7\Delta\delta + K_8\Delta E'_q + K_9\Delta V_{dc} + K_{10}\Delta m + K_{11}\Delta\delta_b \tag{3.20}$$

where

$$\Delta Pe = K_1\Delta\delta + K_2\Delta E'_q + K_{pdc}\Delta V_{dc} + K_{pm}\Delta m + K_{p\delta}\Delta\delta_b$$

$$\Delta E'_q = K_3\Delta\delta + K_4\Delta E'_q + K_{qdc}\Delta V_{dc} + K_{qm}\Delta m + K_{q\delta}\Delta\delta_b$$

$$\Delta V_t = K_5\Delta\delta + K_6\Delta E'_q + K_{vdc}\Delta V_{dc} + K_{vm}\Delta m + K_{v\delta}\Delta\delta_b$$

From equations (3.16)-(3.20), we can obtain the linearised model of the power system, equipped with SSSC.

Fig. 3.3 shows the small signal transfer function block diagram of a single machine infinite bus system including SSSC relating the variables of electric toque, speed, load angle, terminal voltage, field voltage, SSSC control parameters and dc link voltage. This model has been obtained from basic Heffron Phillips model by including dynamics of SSSC.

The significant control parameters of SSSC are:

i.   m - modulation index of the inverter. By controlling m, the magnitude of series injected voltage can be controlled, there by controlling the reactive power compensation.

ii. δ_b – Phase angle of the inverter which when controlled results in real power exchange
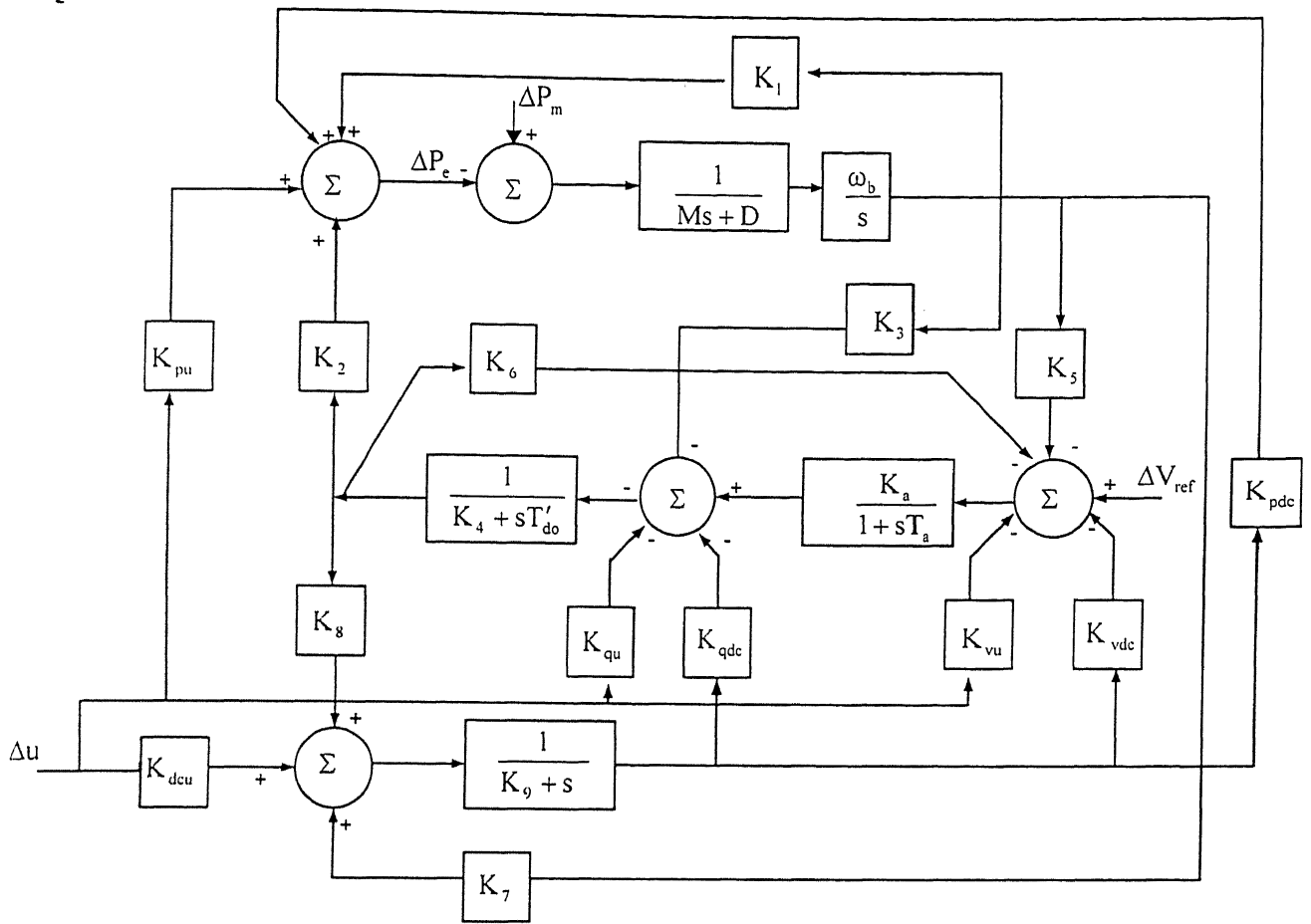
Fig. 3.3 Phillips - Heffron model of single machine infinite bus power system installed with SSSC

3.2 Performance of System Without Any Damping Controller

Modified Phillips - Heffron model of single machine infinite bus power system simulated without any damping controller i.e., $\Delta u = 0$. Response of the system is shown in Fig. 3.4

Table 3.1 Eigen values of system without any damping controller:

Load (p.u)	Without controller
0.8	$0.2721 \pm j\,7.0132$
0.2	$0.0202 \pm j\,6.1994$
1.2	$0.3992 \pm j\,6.6351$
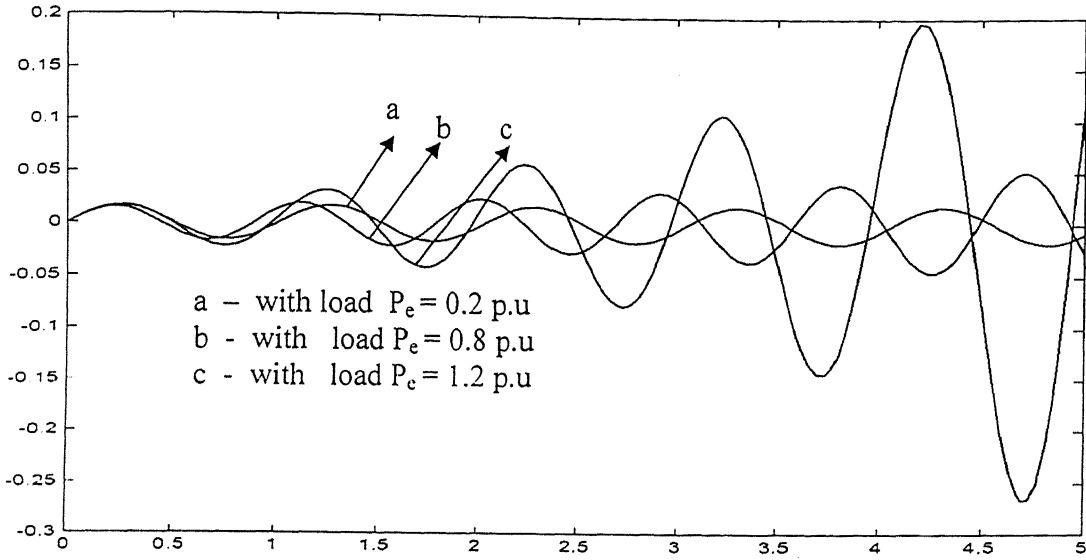
Fig. 3.4 Response of system without any damping controller

Eigen value analysis and simulation results shows that system is unstable for sudden change in load or faults. So it requires damping controller to stabilize the system.

3.3 Design of Damping Controller:

The damping controllers are designed to produce electrical torque in phase with the speed deviation. The two control parameters of SSSC (*i.e.*, m and δ_b) can be modulated in order to produce the damping toque. The speed deviation $\Delta\omega$ is considered as the input to the damping controllers. Effectiveness of two alternative SSSC based damping controllers are examined in the present work.

Damping controller based on SSSC control parameter **m** shall henceforth by denoted as **m**. Similarly damping controller based on δ_b shall henceforth be denoted as δ_b.
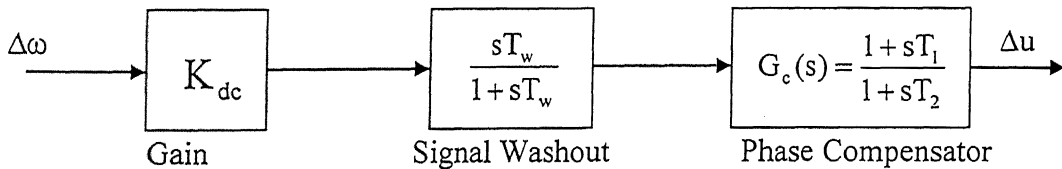
Fig.3.5 Simplified block diagram of SSSC damping controller

32
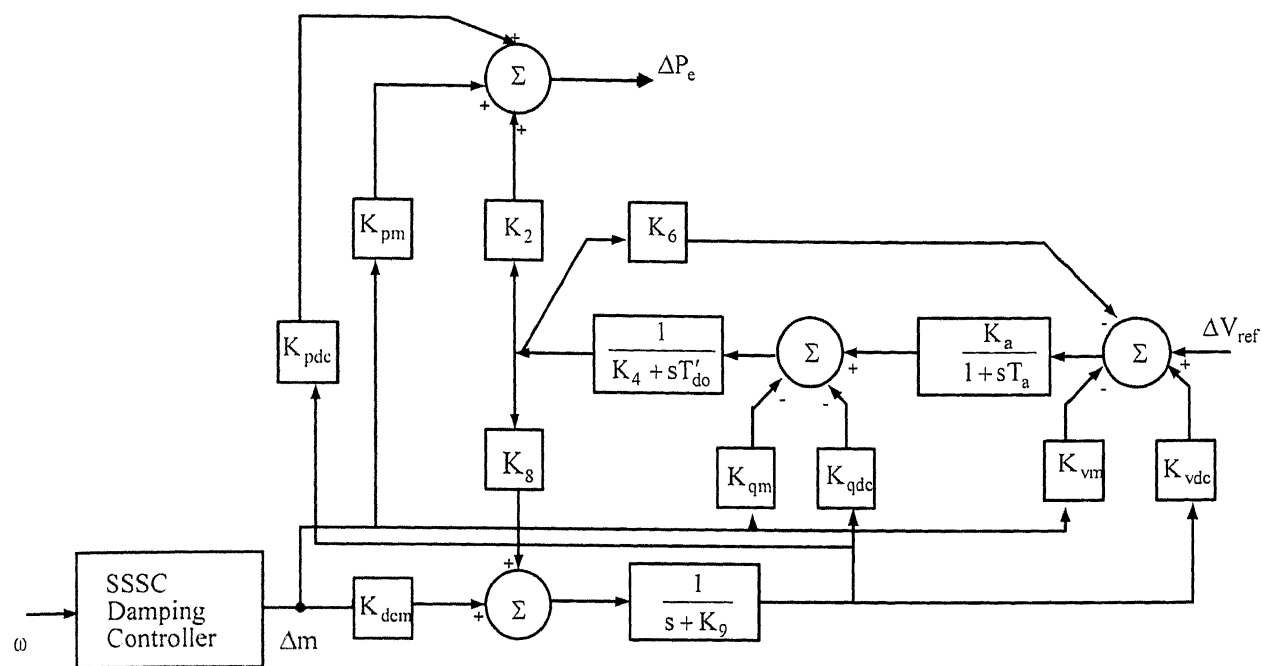
Fig. 3.6 Transfer function of the system relating component of electrical power ($\Delta \underline{P}$) produced by damping controller (Δm).

Fig.3.7 Transfer function of the system relating component of electrical power (ΔP) produced by damping controller ($\Delta \delta_b$).

The structure of the SSSC based damping controller is shown in Fig 3.5. It consists of gain, signal wash out and phase compensation blocks. The parameters of damping controller are obtained by using phase compensation technique. The step by step procedure for obtaining the parameters of the damping controller using phase compensation technique is given below.

1) Computation of natural frequency of oscillations.

2) Computation of phase relation between $\Delta\omega$ and ΔP_e at $s=j\omega_n$

   It can be obtained from the transfer function between ΔP and controlling parameter, transfer function between these parameters can be obtained by reducing the block diagrams of Fig 3.6 & 3.7 for Δm & $\Delta\delta_b$ respectively.

3) Design of phase lead/lag compensator $G_c(s)$.

   The phase lead/lag compensator is designed to provide the required degree of compensation. For 100% of compensation

$$\angle G_c(j\omega_n) + \angle G_p(j\omega_n) = 0 \tag{3.21}$$

Assuming one lead/lag network, $T_1 = a\,T_2$

The transfer function of the compensator becomes

$$G_c(s) = \frac{1 + saT_2}{1 + sT_2} \tag{3.22}$$

Since phase angle compensated by lead/lag network is $-\gamma$, the parameters a, T_1, T_2 are calculated as

$$a = \frac{1 + \sin\gamma}{1 - \sin\gamma}$$

$$T_2 = \frac{1}{\sqrt{\omega_n a}} \tag{3.23}$$

$$T_1 = aT_2$$

4) Computation of optimum gain K_{dc}

   Gain required for desired value of $\zeta = 0.5$ is

34

$$K_{dc} = \frac{2\varsigma \omega_n M}{|G_p||G_c|}$$

(3.24)

3.3.1 Design of damping controller at nominal load P_e=0.8 p.u

Parameters of system under study are given in Appendix – I

Calculation of initial conditions:

$$P_e = \frac{V_t V_b}{X} \sin \theta_o$$

$$I\angle\phi_o = \frac{\overline{V}_t - V_b}{jX}$$

$$E_{qo}\angle\delta_o = V_t\angle\theta_o + jX_q\overline{I}$$

$$i_{do} = I\sin(\delta_o - \phi_o)$$

$$i_{qo} = I\cos(\delta_o - \phi_o)$$

$$E_{fdo} = E_{qo} + (X_d - X_q)i_{do}$$

$$E'_{do} = -(X_d - X'_d)i_{qo}$$

$$E'_{qo} = E_{fdo} - (X_d - X'_d)i_{do}$$

$$\delta_{bo} = \phi_o \mp 90°$$

(3.25)

K –constants of modified Hefron –Philips model are computed using expressions given in Appendix-IV.

$$\dot{x} = Ax + Bu$$

$$x = \begin{bmatrix} \Delta\delta \\ \Delta\omega \\ \Delta E'_q \\ \Delta E_{fd} \\ \Delta V_{dc} \end{bmatrix} \qquad u = \begin{bmatrix} \Delta m \\ \Delta\delta_b \end{bmatrix}$$

Matrices A, B are given in Appendix-III

Oscillating modes of the system without any damping controller at load $P_e = 0.8$ p.u are $0.2721 \pm j\,7.0132$. It shows that system is unstable.

3.3.1.1 Design of damping controller at nominal load P_e=0.8 p.u. considering Δm as controlling parameter

$$\dot{x} = A_m x + B_m u$$

A_m and B_m are given in Appendix-III

Above state space representation can be represented as block diagram Fig .3.6

Transfer function of the system is obtained by block diagram reduction of Fig. 3.6.

Transfer function at $s = j\omega_n$, $G_p = 0.8406 - j0.1836$

From above

$$\gamma = 12.32°$$

$$a = \frac{1 + \sin \gamma}{1 - \sin \gamma} = 1.542$$

$$T_2 = \frac{1}{\sqrt{\omega_n a}} = 0.115$$

$$T_1 = aT_2 = 0.1774$$

then

$$Gc\,(s) = 1.542 \frac{s + 5.637}{s + 8.695}$$

$$Gc(\,j\omega_n\,) = 1.24\angle 12.32$$

Assuming ζ=0.5

$$K_{dc} = \frac{2\varsigma\omega_n M}{|G_p||G_c|} = 52.5$$

3.3.1.2 Design of damping controller at nominal load P_e=0.8 p.u. considering $\Delta\delta$ as controlling parameter

Parameters of system under study are given in Appendix – I

$$\dot{x} = A_{\delta b} x + B_{\delta b} u$$

$A_{\delta b}$ and $B_{\delta b}$ are given in Appendix-III

Above state space representation can be represented as block diagram Fig. 3.7

Transfer function of the system is obtained by block diagram reduction of Fig. 3.7
Similar to 3.3.1.1, damping controller considering $\Delta\delta_b$ as controlling parameter is also designed.

$$G_c(s) = 0.725\frac{s+8.196}{s+5.963}$$

$$G_c(j\omega_n) = 1.172\angle-9.1$$

$$K_{dc} = \frac{2\varsigma\omega_n M}{|G_p||G_c|} = 117.69$$

Fig. 3.8 Response of $\Delta\omega$ with Δm and $\Delta\delta_b$ as the controlling parameters at nominal load $P_e=0.8$ p.u

3.4 Performance Evaluation of Damping Controller Designed at Nominal Operating Point for Different Loading Conditions

In any power system, the operating load varies over a wide range. It is extremely important to investigate the effect of variation of the loading condition on the dynamic response of the system. In order to examine the robustness of the damping controller to wide variation in the loading condition, loading of the system is varied over a wide range ($P_e=0.2$ p.u to $P_e=1.2$ p.u.) and dynamic responses are obtained for each of the loading condition. The parameters of damping controllers are computed at nominal operating condition for the step perturbation in mechanical power ($\Delta P_m=0.01$ p.u).

3.4.1 Investigating response of $\Delta\omega$ at load P_e=0.2 p.u.

Calculation of initial conditions:

Parameters of system under study are given in Appendix – I

Initial conditions are computed using expressions in equation (3.25)

K –constants of modified Hefron –Philips model are computed using expressions given in Appendix-IV

$$\dot{x} = Ax + Bu$$

Matrices A, B are given in Appendix-III

Oscillating modes of the system without any damping controller are $0.0202 \pm j\,6.1994$.
It shows that system is unstable

      Above state space representation of system is simulated using MATLAB simulink with damping controller designed at nominal operating point considering Δm and $\Delta\delta_b$ separately.

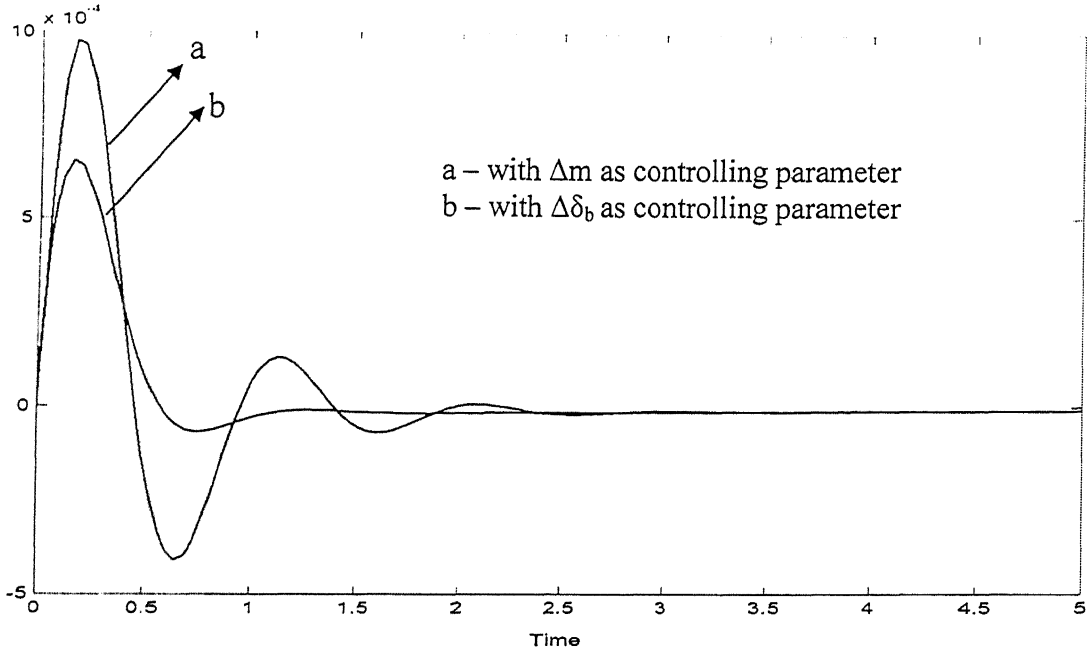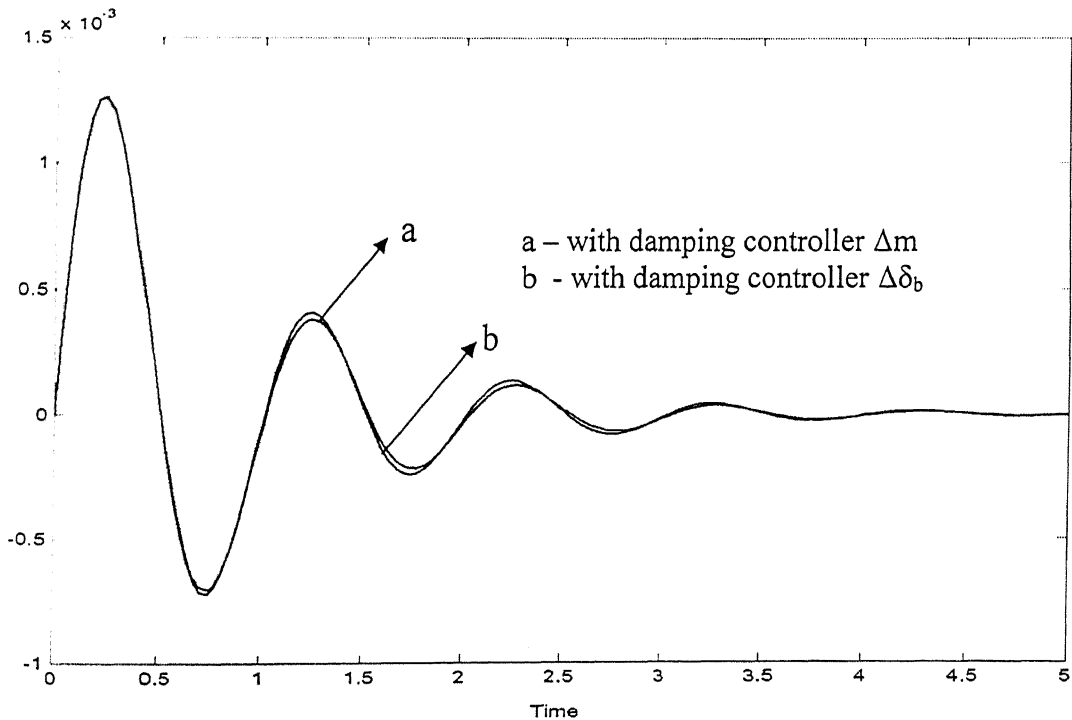

Fig. 3.9 Response of $\Delta\omega$ with Δm and $\Delta\delta_b$ as the controlling parameters at load P_e=0.2 p.u.

3.4.2 Investigating response of $\Delta\omega$ at Load P_e=1.2 p.u

Calculation of initial conditions:

Parameters of system under study are given in Appendix – I

Initial conditions are computed using equation (3.25)

K –constants of modified Hefron –Philips model are computed using expressions given in Appendix-IV

$$\dot{x} = Ax + Bu$$

Matrices A, B are given in Appendix-III

$$x = \begin{bmatrix} \Delta\delta \\ \Delta\omega \\ \Delta E'_q \\ \Delta E_{fd} \\ \Delta V_{dc} \end{bmatrix} \qquad u = \begin{bmatrix} \Delta m \\ \Delta\delta_b \end{bmatrix}$$

Oscillating modes of the system without any damping controller are $0.3992 \pm j\,6.6351$. It shows that system is unstable.

Above state space representation of system is simulated using MATLAB simulink with damping controller designed at nominal operating point considering Δm and $\Delta\delta_b$ separately.
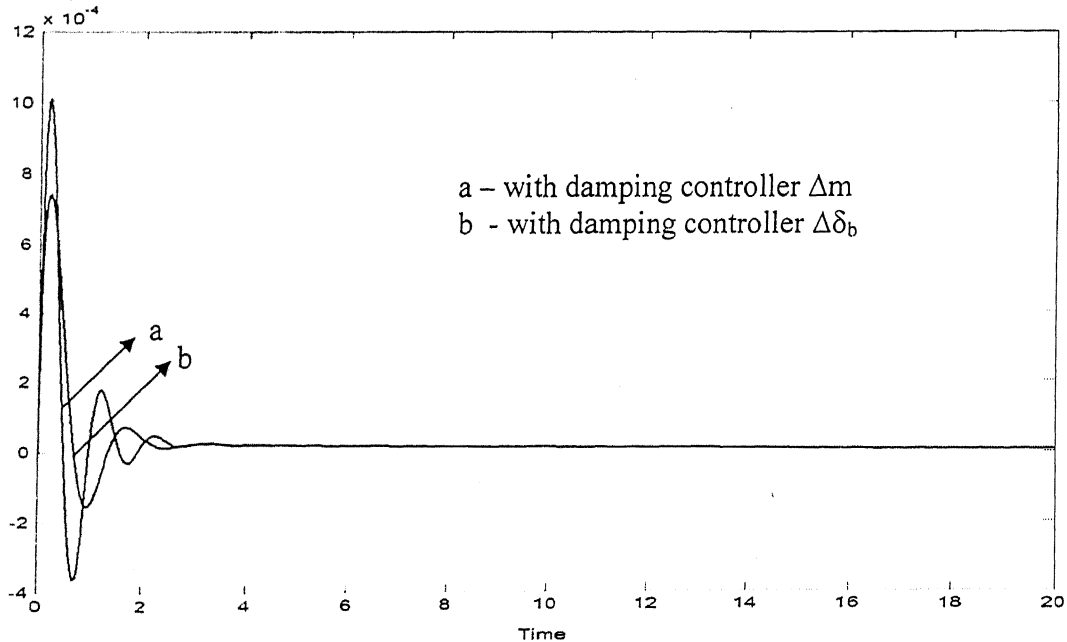
Fig 3.10 Response of $\Delta\omega$ with Δm and $\Delta\delta_b$ as the controlling parameters at load P_e=1.2 p.u

39
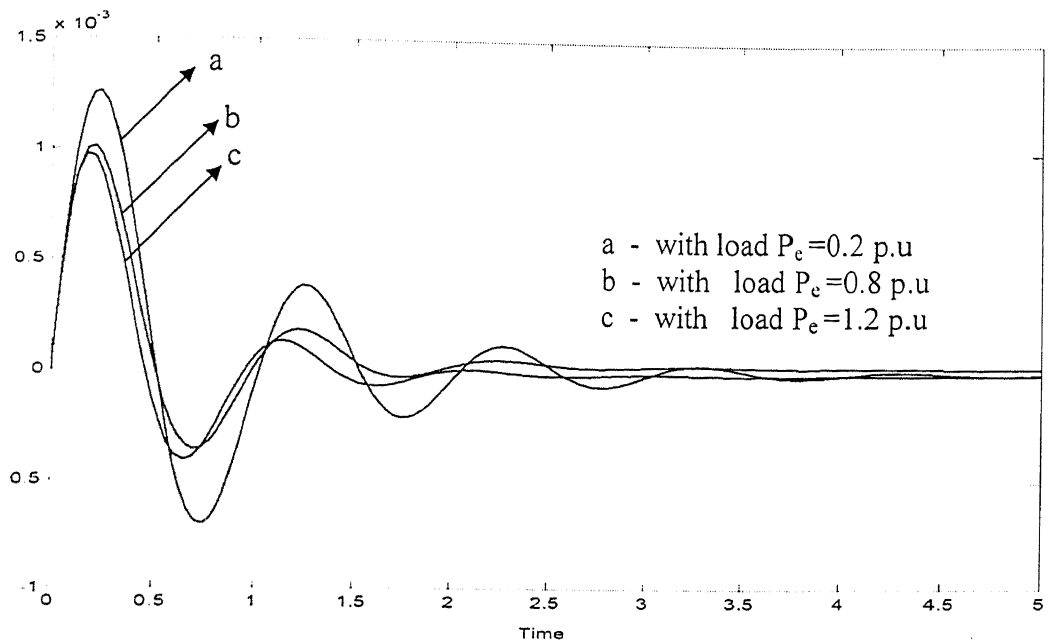
Fig 3.11 Response of Δω with controlling parameter Δm at different loads
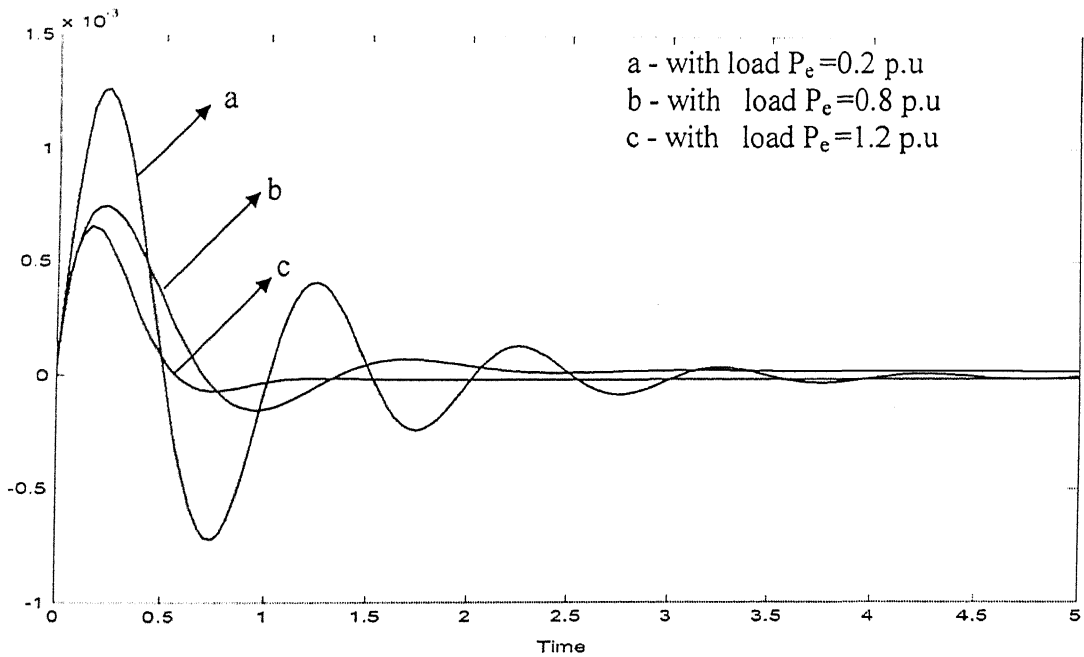
Fig 3.12 Response of Δω with controlling parameter $\Delta\delta_b$ at different loads

Form figs.3.8-3.12 we can easily conclude that damping controller $\Delta\delta_b$ is more effective in damping low frequency oscillations than the damping controller Δm.

3.5 Selection of Operating Point for Designing Damping Controller for Robust Performance

From Figs 3.11-3.12 we can conclude that effectiveness of the SSSC based stabiliser changes with variation of power system operating condition and with both the damping controllers response at light load condition deteriorates significantly compared to the response at nominal load. To guarantee the robustness of the SSSC based stabiliser over a set of known operating conditions, we should choose the operating condition at which the SSSC based stabiliser is least effective so that once the controller is designed at that operating condition properly, it can work effectively over a wide range of operating conditions. In the present case, the SSSC based damping controller is least effective at operating condition P_e =0.2 p.u, hence it is proposed to design damping controller corresponding to this operating condition. Henceforth, this operating point called as robust operating point. Superior response of damping controller designed at robust operating point is indicated by eigen values of system and by comparing the simulation results with damping controller designed at this operating point shown in Figs 3.13 & 3.14 with simulation results shown in Figs. 3.11 & 3.12.

Eigen values of the system without damping controller and with damping controller Δm are shown in Table 3.2.

Table 3.2 Eigen value analysis with Δm as controlling parameter.

Load	Without controller	controller designed Δm based on nominal load	Controller designed at robust operating point
0.8	$0.2721 \pm j\,7.0132$	$-2.8854 \pm j\,7.4447$	$-5.3353 \pm j\,7.7201$
0.2	$0.0202 \pm j\,6.1994i$	$-1.8067 \pm j\,6.4030$	$-2.9467 \pm j\,6.4134$
1.2	$0.3992 \pm j\,6.6351$	$-3.7094 \pm j\,6.7909$	$-8.0509 \pm j\,6.0186$

Eigen values of the system without damping controller and with damping controller $\Delta \delta_b$ are shown Table 3.3

Table 3.3 Eigen value analysis with $\Delta \delta_b$ as controlling parameter

| Load	Without controller	controller designed at nominal load P_e =0.8	Controller designed at robust operating point P_e =0.2
0.8	$0.2721 \pm j\,7.0132$	$-13.2111 \pm j\,17.0949$	$-27.2139 \pm j\,30.3072$
0.2	$0.0202 \pm j\,6.1994$	$-0.8817 \pm j\,6.1080$	$-3.0225 \pm j\,5.2614$
1.2	$0.3992 \pm j\,6.6351$	$-1.6422 \pm j\,5.2643$	$-3.1936 \pm j\,2.0010$ $-67.2248 \pm j\,22.2619$
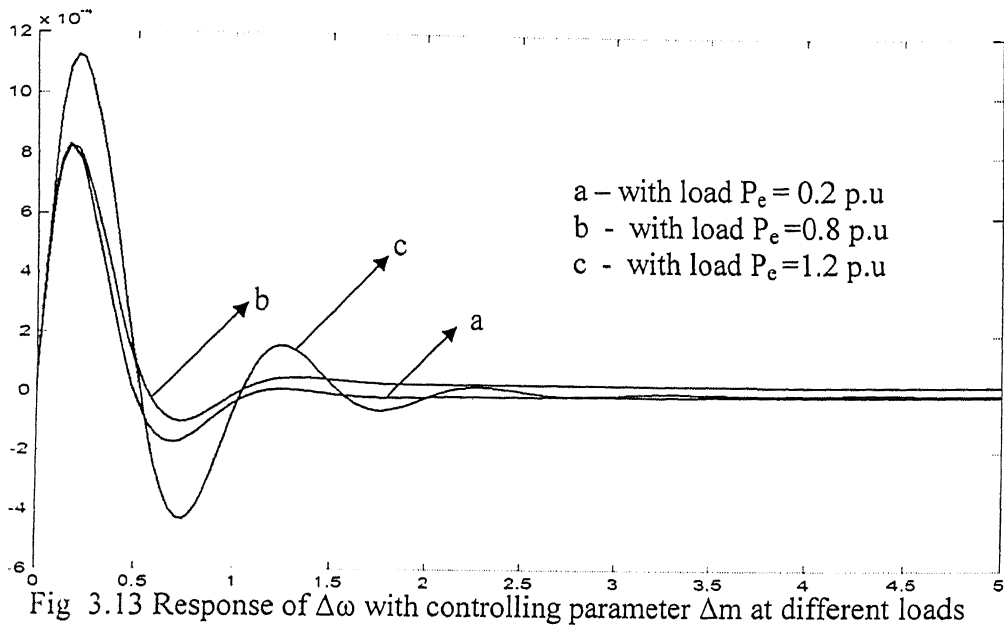
Fig 3.13 Response of $\Delta\omega$ with controlling parameter Δm at different loads
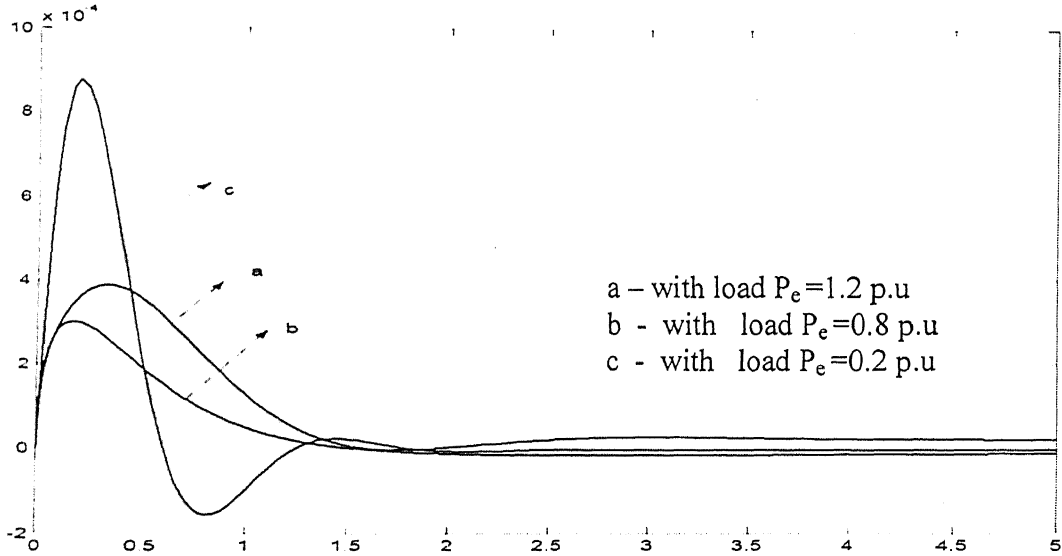
Fig 3.14 Response of $\Delta\omega$ with controlling parameter $\Delta\delta_b$ at different loads

Fig.3.13 shows response of $\Delta\omega$ with damping controller Δm designed at robust operating condition. It is clearly seen that dynamic performance deteriorates slightly at light load condition compared to the response at nominal loading.

Fig. 3.14 shows response of $\Delta\omega$ with damping controller $\Delta\delta_b$ designed at robust operating condition. It is clearly seen that dynamic performances are hardly affected in terms of settling time following wide variations in loading condition.

42

From the above studies, it can be concluded that the damping controller δ_b exhibits robust performance compared to the damping controller m.

3.6 Performance of the Damping Controllers with Variation in System Parameters

Dynamic performance of damping controllers designed at robust operating condition can be investigated under wide variations of equivalent reactance. Variation in equivalent reactance is may be due to change in network configuration by switching of transmission lines or generators.
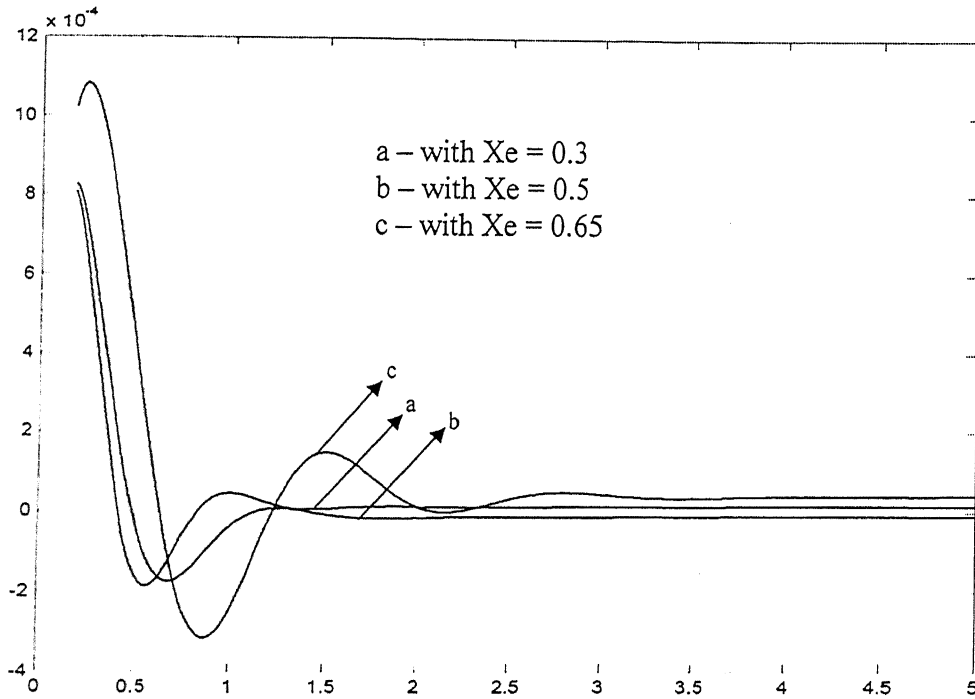
Fig 3.15 Response of $\Delta\omega$ with controlling parameter Δm at different values of equivalent reactance.

Fig. 3.15 shows response of $\Delta\omega$ with damping controller Δm designed at robust operating condition. It is clearly seen that dynamic performance deteriorates slightly at higher values of equivalent reactance (Xe) compared to the response at nominal value of Xe.

Fig. 3.16 shows response of $\Delta\omega$ with damping controller $\Delta\delta_b$ designed at robust operating condition. It is clearly seen that dynamic performances are hardly affected in terms of settling time following wide variation in Xe compared to the response at nominal value of Xe.

43
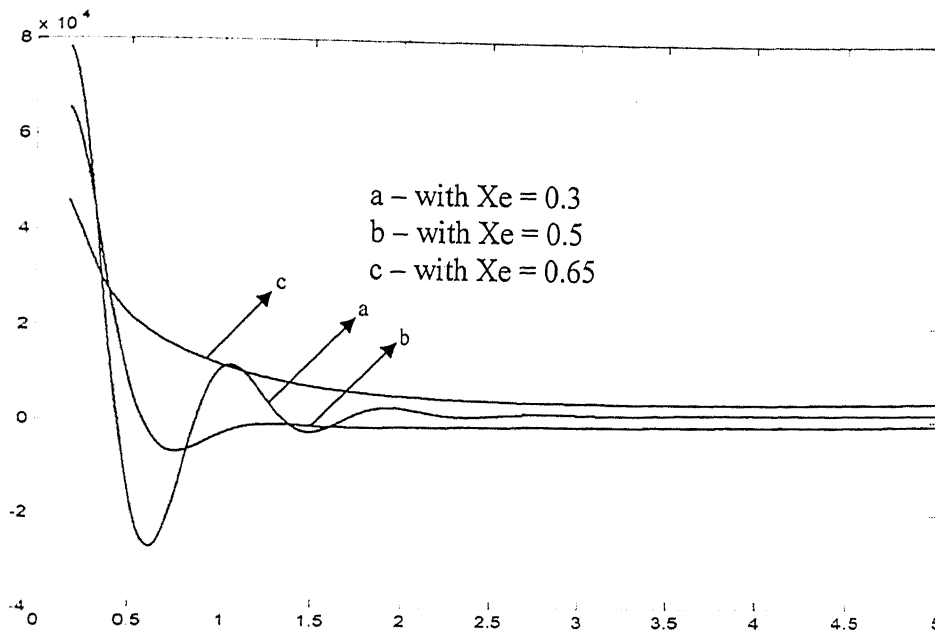
Fig 3.16 Response of $\Delta\omega$ with controlling parameter $\Delta\delta_b$ at different values of equivalent reactance.

3.7 Conclusions

From the eigen analysis and results of simulation we can confirm the robustness of the controller designed at robust operating condition. It may concluded that damping controller (δ_b) is quite robust to wide variation in operating condition and system parameters. The reason for the superior performance of damping controller (δ_b) may be attributed to the fact that modulation of δ_b results in exchange of real power.

A systematic approach for designing SSSC based damping controller for damping out power system low frequency oscillations and the selection of robust operating condition to achieve robust performance of the damping controller is presented.

The performance of two alternate damping controllers has been examined considering the wide variation in operating condition and line reactance Xe.

Investigation reveals that the damping controller δ_b provide robust performance to wide variation in loading condition and line reactance Xe. It may thus be recommended that the damping controller based on SSSC should be designed corresponding to robust operating condition and control parameters δ_b may be preferred over the control parameter m.

44

CHAPTER 4

APPLICATION OF THE DESIGNED SSSC BASED DAMPING CONTROLLER IN A PRACTICAL SYSTEM

In this Chapter, the SSSC based damping controller designed in Chapter 3 is implemented on a part of Indian power system. System taken for the study is shown in Fig. 4.1. It is the part of TALA transmission system assuming that an SSSC is installed at Purnia, Bihar. Though this study is on Single machine infinite bus model, it can be extended to multi-machine system as well. Without the damping controller, one of the modes is oscillating due to poor damping. It means that, if the power system had disturbance such as short circuit, the power flow will oscillate with low frequency. These oscillations will be more at lightly loaded conditions. In this Chapter, the SSSC based damping controller is designed at an operating point as selected similar to that in Chapter 3 to give robust performance. This operating point, henceforth, termed as robust operating point. Effectiveness of controlling parameters Δm and $\Delta \delta_b$ are investigated at different loading conditions. The performance of controlling parameters at varying system parameters is also investigated.

4.1 Modeling of the System with SSSC

Modeling of the system is same as that given in Chapter 3. Parameters of the system are given in Annexure II. From Chapter 3, the system can be described by following equations.

$$\Delta \dot{\delta} = \omega_b \Delta \omega$$
$$\Delta \dot{\omega} = \left(- \Delta P_e - D\Delta \omega \right) / M$$
$$\Delta \dot{E}'_q = \left(- \Delta E_q + \Delta E_{fd} \right) / T'_{do}$$
$$\Delta \dot{E}_{fd} = -\frac{1}{T_A} \Delta E_{fd} + \frac{K_A}{T_A} \left(- \Delta V_t \right)$$
$$\dot{V}_{dc} = K_7 \Delta \delta + K_8 \Delta E'_q + K_9 \Delta V_{dc} + K_{10} \Delta m + K_{11} \Delta \delta_b$$

where

$$\Delta Pe = K_1 \Delta \delta + K_2 \Delta E'_q + K_{pdc} \Delta V_{dc} + K_{pm} \Delta m + K_{p\delta} \Delta \delta_b$$
$$\Delta E'_q = K_3 \Delta \delta + K_4 \Delta E'_q + K_{qdc} \Delta V_{dc} + K_{qm} \Delta m + K_{q\delta} \Delta \delta_b \qquad (4.1)$$
$$\Delta V_t = K_5 \Delta \delta + K_6 \Delta E'_q + K_{vdc} \Delta V_{dc} + K_{vm} \Delta m + K_{v\delta} \Delta \delta_b$$
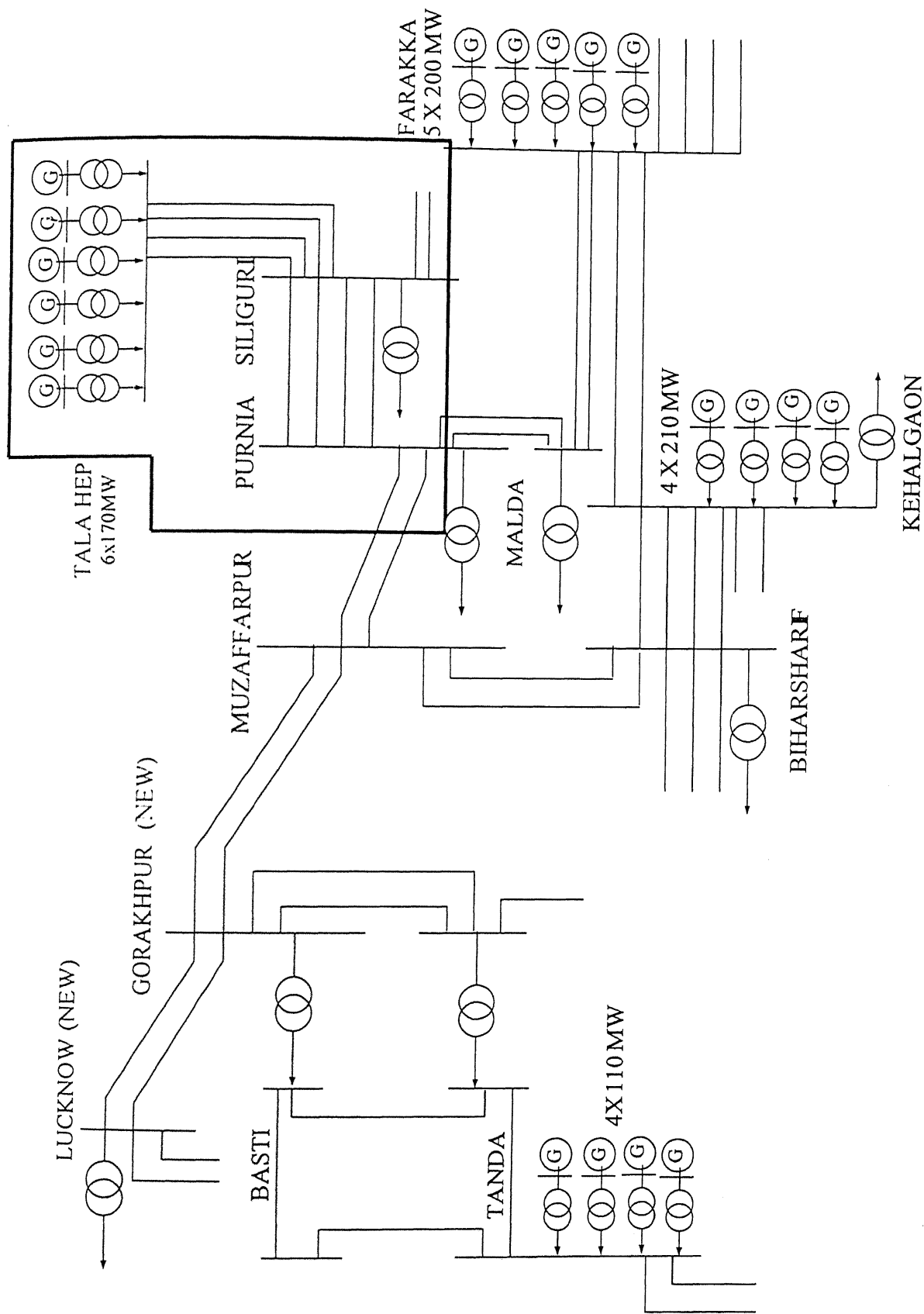
Fig. 4.1 Part of the system taken for implementing SSSC based damping controller

46

With Δm as controlling parameter, $K_{p\delta}$, $K_{q\delta}$, $K_{v\delta}$ become zero.

With $\Delta\delta_b$ as controlling parameter, K_{pm}, K_{qm}, K_{vm} are equal to zero.

State space representation of above equations is as follows.

$$\dot{x} = Ax + Bu$$

$$x = \begin{bmatrix} \Delta\delta \\ \Delta\omega \\ \Delta E'_q \\ \Delta E_{fd} \\ \Delta V_{dc} \end{bmatrix} \qquad u = \begin{bmatrix} \Delta m \\ \Delta\delta_b \end{bmatrix}$$

Matrices A, B are given in Annexure-I

Table 4.1 Eigen values of SSSC compensated power system

Load(p.u.)	Without controller
S=0.8+j0.1	-26.26 ± j 38.45 **0.1132 ± j9.99** -0.0311
S=0.2+j0.01	-26.1272 ± j 32.5 **0.0031 ± j 7.8948** -0.0032
S=1.2+j0.4	-26.42 ± j 45.89 **0.2698 ± j13.2793** -0.005

From eigen values in Table 4.1 show that the system is unstable. If there is any disturbance in the system, the power flow in the system will oscillate at frequency around 1 to 2 Hz. Response of system without any damping controller is shown in Fig.4.2

4.2 Design of Damping Controller

To provide damping to the oscillating mode, the damping controller is designed using phase compensation technique. From Chapter 3, we can choose S = 0.2 + j 0.01 p.u as robust operating condition for designing damping controller. By using phase compensation method SSSC based damping controller with Δm as control parameter, the controller is designed at the

operating point S = 0.2 + j 0.01 p.u. The response at different loading conditions are shown in Fig 4.3.
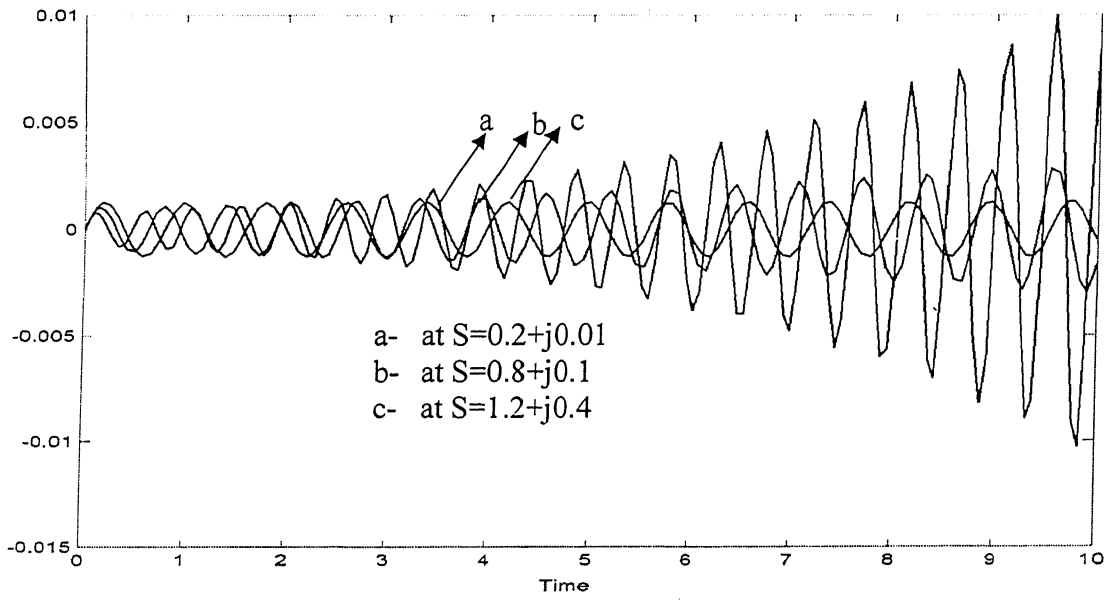
Fig 4.2: Response of Δω without any damping controller

Transfer function of the designed controller is

$$G_c(s) = 132.43 \frac{s + 4.63}{s + 13.2}$$

By using phase compensation method SSSC based damping controller with $\Delta\delta_b$ as controlling parameter, the controller is designed at operating point S = 0.2 + j 0.01 p.u. The responses at different loading conditions are shown in Fig. 4.4.

Transfer function of the designed controller is

$$G_c(s) = 52.5 \frac{s + 7.89}{s + 7.01}$$

4.3 Investigation of Effectiveness of Damping Controllers at Different Loading Conditions

To investigate effectiveness of damping controllers at different loading conditions, damping controllers are designed for different controlling parameters separately and the system under study is simulated at different loading conditions with each damping controller.

4.3.1 Effectiveness of damping controller Δm at different loading conditions

System under study is simulated at different loading conditions (i.e S=0.2+j0.01 p.u, S=0.8+j0.1 p.u. and S=1.2+j0.4 p.u.). The damping controller is designed at S=0.2+j0.01 p.u. for controlling parameter Δm to investigate the effectiveness of controlling parameter Δm at different loading conditions. Response of system with damping controller Δm is shown in Fig.4.3
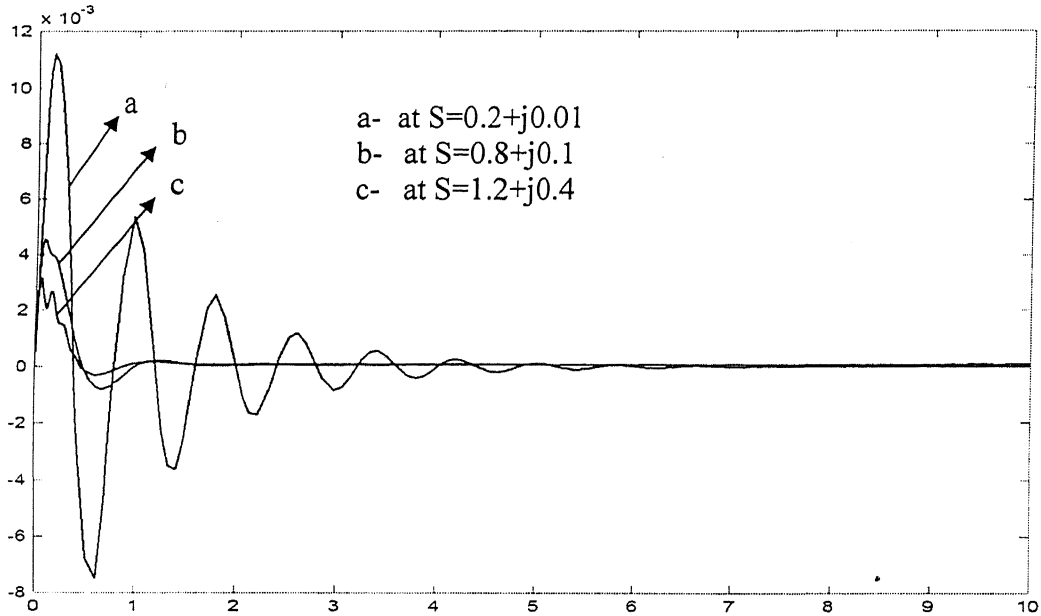
Fig. 4.3: Response of Δω at different loading conditions with Δm as controlling parameter

4.3.2 Effectiveness of damping controller $\Delta\delta_b$ at different loading conditions

System under study is simulated at different loading conditions (i.e S=0.2+j0.01 p.u, S=0.8+j0.1 p.u and S= 1.2+j0.4 p.u). The damping controller is designed at S=0.2+j0.01 p.u for controlling parameter $\Delta\delta_b$ to investigate the effectiveness of controlling parameter $\Delta\delta_b$ at different loading conditions. Response of system with damping controller $\Delta\delta_b$ is shown in Fig. 4.4

From Fig 4.3, 4.4, we can conclude that the damping controller designed at robust operating condition will give good response over wide range of operating conditions

Fig.4.4: Response of $\Delta\omega$ at different loading conditions with $\Delta\delta_b$ as controlling parameter

4.4 Comparison of Effectiveness of Damping Controllers

Since there are two controlling parameters, it is necessary to compare the effectiveness of controlling parameters and design the damping controller based on most effective controlling parameter for wide variations in loading and variations in system parameters.

4.4.1 Comparison of effectiveness of damping controllers at S=0.8+ j 0.1 p.u

System with loading S=0.8+j0.1 p.u simulated with both damping controllers designed at robust operating point.
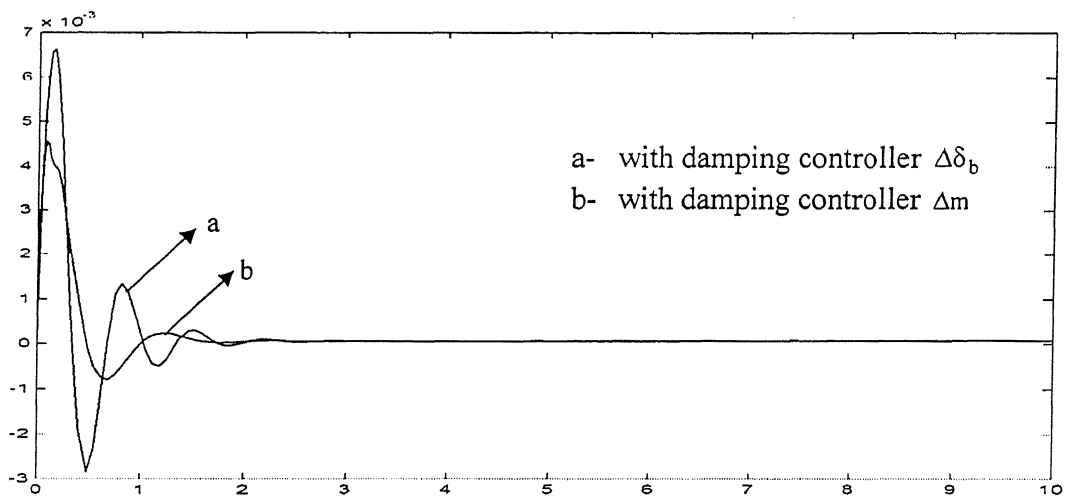
Fig:4.5 Response of $\Delta\omega$ with different controlling parameters at loading S = 0.8+ j 0.1 p.u.

4.4.2 Comparison of effectiveness of damping controllers at S= 0.2 + j 0.01 p.u.

System with loading S=0.2+j0.01 p.u. is simulated with both damping controllers designed at the robust operating point.
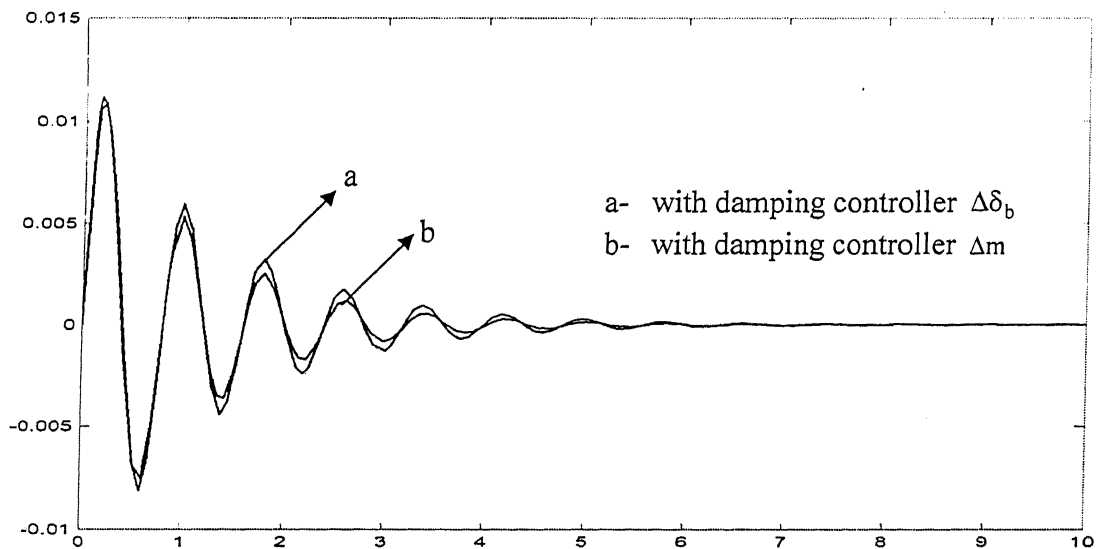
Fig:4.6 Response of $\Delta\omega$ with different controlling parameters at loading S = 0.2+ j 0.01 p.u.

4.4.3 Comparison of effectiveness of damping controllers at S= 1.2+ j0.4 p.u.

System with loading S=1.2+j0.4 p.u. is simulated with both damping controllers designed at the robust operating point.
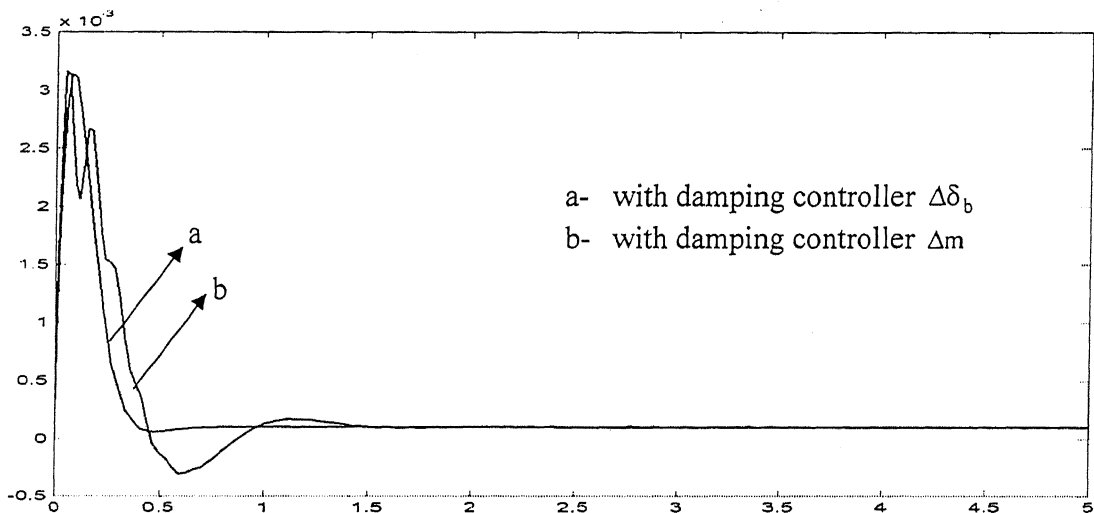
Fig: 4.7 Response of $\Delta\omega$ with different controlling parameters at loading S = 1.2+ j 0.4 p.u.

From Figs. 4.5, 4.6, 4.7, the response of $\Delta\omega$ at S = 0.2+j0.01 p.u. and at S=0.8+j0.1 p.u. with different damping controllers are almost same, there is no difference in terms of setting time with different damping controllers, but at loading S=1.2+j0.4 p.u. The response of $\Delta\omega$ with $\Delta\delta_b$ settles far earlier than that of with Δm. In overall, we can say that the response of damping controller $\Delta\delta_b$ is superior than that with damping controller Δm.

4.5 Performance Evaluation for Varying System Parameter Condition

Variation of system parameters in a practical system is common due to tripping of transmission lines or generators or due to forced/ planned outages. In the present case, one of the lines of double circuit transmission line from Siliguri to Purnia is taken under outage as a result net reactance of the line increases, at this condition effectiveness of damping controller designed at robust operating condition was investigated and response is shown in Fig. 4.8.
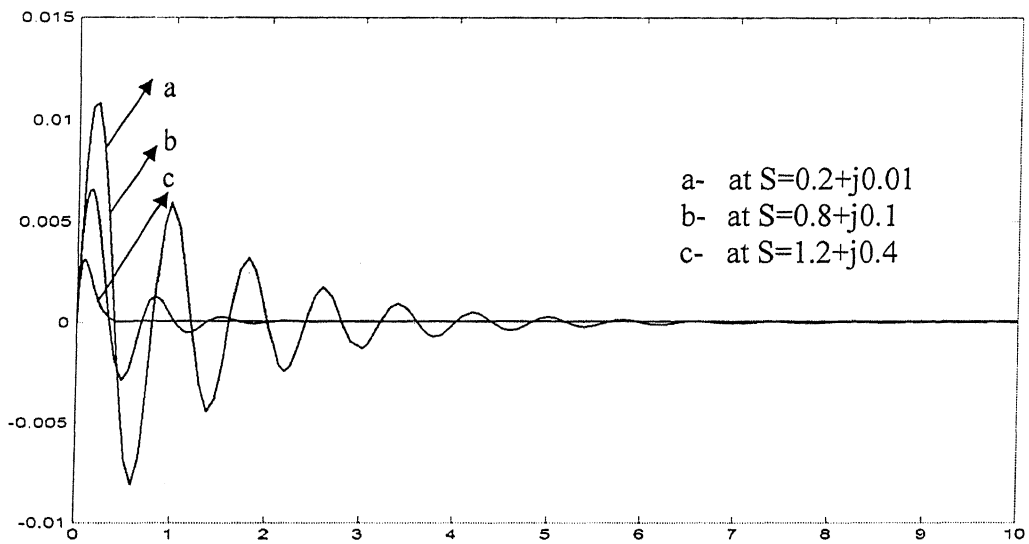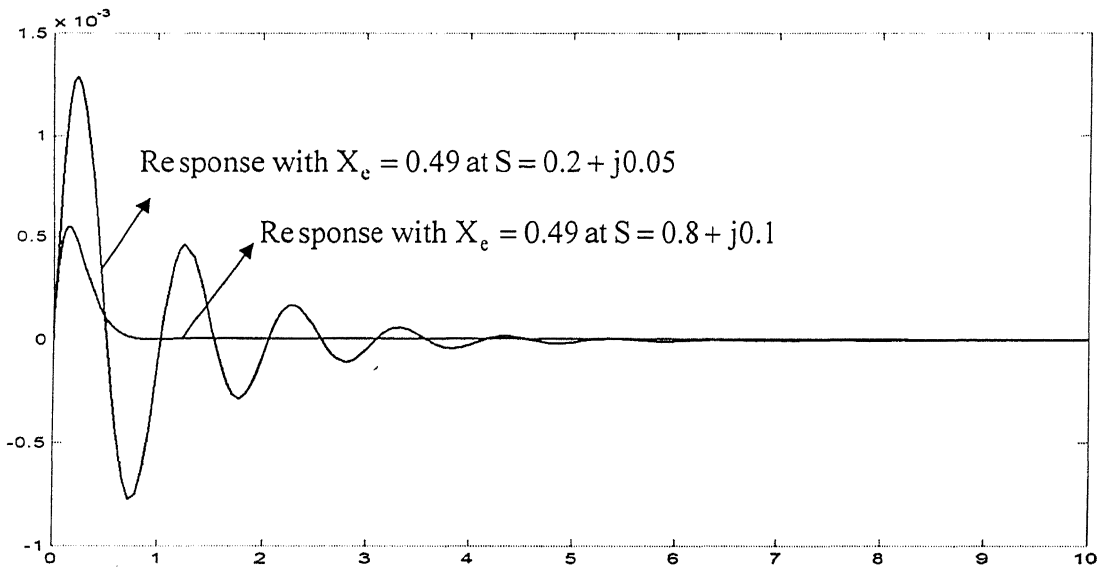

Fig.4.8: Response of $\Delta\omega$ at different loading conditions with $\Delta\delta_b$ as controlling parameter with one of D/C line outage.

4.6 Conclusions

From results of simulation, we can confirm the robustness of the controller designed at robust operating condition. It may be concluded that damping controller (δ_b) is quite robust to wide variation in operating condition and system parameters. The reason for the superior performance of damping controller (δ_b) may be attributed to the fact that modulation of δ_b results in exchange of real power.

A systematic approach for designing SSSC based damping controller for damping power system low frequency oscillations and selection of robust operating condition to achieve robust performance of the damping controller, as presented in Chapter 3, is applied to a part of practical Indian system. It is observed that the controller provides sufficient damping to the oscillating mode.

The performance of two alternate damping controllers has been examined considering the wide variation in operating condition and equivalent reactance Xe.

Investigation reveals that the damping controller δ_b provides robust performance to wide variation in loading condition and line reactance Xe. It may thus be recommended that the damping controller based on SSSC may be designed corresponding to robust operating condition and control parameters δ_b may be preferred over the control parameter m.

CHAPTER 5

CONCLUSIONS

5.1 Contributions of the Present Work

A systematic approach for designing SSSC based damping controller for damping power system oscillations has been presented.

The performance of two damping controllers, damping controller m (Amplitude modulation index) and damping controller δ_b (Phase angle of output voltage of inverter) has been examined considering wide variations in loading conditions and line reactance Xe.

Selection of operating point for designing damping controller for robust performance has been presented and verified by applying proposed procedure of designing damping controller to a practical system.

5.2 Scope for Future Research Work

1. Proposed procedure for designing SSSC based damping controller is to be studied in multi machine system.
2. System behavior during balanced or unbalanced faults in power system needs to be investigated.
3. Robust design techniques can be used to design damping controller.

REFERENCES

1. N. G. Hingorani, "High power electronics and flexible AC transmission system," *IEEE Power engineering Review*, July 1998

2. A. Edris, "FACTS Technology Development: An Update," *IEEE Power engineering Review*, March 2000

3. K. N. Zadeh, R.C. Meyer, and G. Cauley, "Practices and new concepts in power system control", *IEEE Trans. on Power Systems,* Vol. 11, No. 1, pp. 3-9, 1996.

4. L. H. Fink and P.J.M. Van Son, "System control with in a restructured industry", IEEE *Trans. on Power Systems*, Vol. 13, No. 2, pp. 611-616,1998.

5. N. Jaleeli, L. S. Vanslyck, D.N Ewart, L.H. Fink, and A. G. Hoffmann, "Understanding automatic generation control," *IEEE Trans. on Power Systems,* vol. 7, No. 3, pp. 1106-1122, 1992.

6. L. Gyugyi, C. D. Schauder, and K. K. Sen, "Static synchronous series compensator: a solid state approach to the series compensation of transmission line", *IEEE Trans. on Power Delivery*, Vol. 12, No. 1, pp. 406-417, 1997.

7. N. G. Hingorani, "A new scheme for sub synchronous resonance damping of torsional oscillations and transient torque" *IEEE Trans. Power App. &Syst.,* Vol PAS-100, No.4, pp. 1852-1855,1981.

8. H. Jiang, J. Dirsey, T. Habetlat, and K.V. Eckroth, "A cost effective generator brake for improved generator transient response," *IEEE Trans. on Power Systems* Vol. 9, No. 4, pp. 1840-1846, 1994.

9. M. M. A. Salama, H. Temraz, A.Y. Chikhani, and M.A. Bayouni, "Fault current limiter with thyristor controlled impedance," *IEEE Trans. Power Delivery*, Vol. 11, No. 1, pp. 406-417, 1996.

10. N. G. Hingorani and L. gyugyi, "Understanding FACTS", *IEEE Press*, New York, 1999.

11. L. Gyugyi, "Reactive power generation and control by thyristor circuits, " *IEEE Trans. on Industrial Applications,* Vol. 1A-15, no. 5, September/October 1979.

12. L. Gyugyi, "A unified power control concept for flexible AC transmission systems," *IEE Proceedings-C*, Vol. 139, No. 4, July 1992.

13. L. Gyugyi, "Dynamic compensation of AC transmission lines by solid state synchronous voltage sources," *IEEE trans. power Delivery*, Vol. 9, No. 2,pp. 904-911, 1994.

14. L. Gyugyi, C. D. Schauder, S. L. Torgerson, and A. Edris, "The Unified power flow controller: A new approach to power transmission control," *IEEE trans Power Delivery,* Vol. 10, no. 2, pp. 1085-1093, 1995.

15. Byung-Moon Han, Hee-Joong Kim, and Seung-Taek Baek, "Performance analysis of SSSC based on three level multi bridge PWM inverter," Electric *Power System Research* 61 pp.195-202, 2002.

16. B. Han, S. Baek, H. Kim, and G. Karady, "Dynamic characteristics of SSSC based on multi-bridge inverter," IEEE *Trans. on Power Delivery* Vol.17, No.2, April 2002.

17. C. Hochgraf and R. H. Lasetter, "A Transformer less static synchronous series compensator employing multi-level inverter," *IEEE Trans. on Power Delivery*, Vol. 10, No.2, pp. 732-738, 1995.

18. R.W. Menziz and Y. Zhuang, "Advanced static compensation using a multi-level GTO thyristor inverter," *IEEE Trans. on Power Electronics*, Vol. 6, pp. 380-391, 1991.

19. L. Sunil Kumar and A. Ghosh, "Modeling and control design of a static synchronous series compensator, " *IEEE Trans. on Power Delivery*, Vol. 14, No.4, pp. 1448-1453, 1999.

20. L. Sunil Kumar and A. Ghosh, "Static synchronous series compensator-design, control and application," *Electric Power System Research*, Vol.49, pp.139-148, 1999.

21. S. Kannan, S. Jayaram, and M. M. A. Salama, "Fuzzy logic based supplementary controller for Static Synchronous Series Compensator," *Proceedings of the 1998 11ᵗʰ Canadian Conference on Electrical and Computer Engineering,* CCECE. Part 2   (of 2), 1998.

22. Jianhong Chen, Tjing T. Lie, and D.M. Vilathgamuwa, "Damping of power system oscillations using SSSC in real time implementation," *Electrical Power and Energy Systems,* Vol. 26, pp.357-364, 2004.

23. H. F. Wang, "Static synchronous series compensator to damp power system oscillations," *Electric power system research,* Vol, 54, pp.113-119, 2000.

24. Y. H. Song and A.T. Johns, "Flexible AC transmission systems (FACTS)," *IEEE Press,* New york.

APPENDIX – I
System Data

Generator Data:

M=8MJ/MVA $\qquad$ T_{do}=5.044 sec

X_d=1 $\qquad$ Xq=0.6

X_d^1=0.3 $\qquad$ D = 0.0

Excitation system data:

Ka=100 $\qquad$ Ta=0.01 sec

Transformer data:

X_{sct} = 0.1

Transmission line data:

X_b=0.3, $\qquad$ X_t =0.1,

$X=X_b+X_t+X_{sct}$=0.5

Operating conditions:

P=0.8, V_t =1, V_b =1, f =50 Hz.

SSSC parameters:

SSSC parameters are calculated assuming SSSC provides 50% capacitive compensation.

DC link parameters:

V_{dc} =1, C_{dc} =1

DC link capacitor $\qquad$ 2000μF

* All dimensions are in p.u except indicated.

APPENDIX – II
Practical System Data

Transmission line data:

S.no	Transmission line	Length (km)	Conductor type
1	Tala – siliguri 400 kV D/C line -I	90	Twin Moose
2	Tala – siliguri 400 kV D/C line -II	120	Twin Moose
3	Siliguri- Purnia 400 kV D/C line -I	250	Twin Moose
4	Siliguri- Purnia 400 kV D/C line -II	162	Quad Moose

S.no	Conductor type	Resistance (ohm/km)	Reactance (ohm/km)	Susceptance (micro ohm/km)
1	Twin Moose	0.02979	0.332	3.469
2	Quad Moose	0.0146	0.2509	4.623

Generator data:

Rated apparent power	1200MVA
Rated voltage	13.8 kV
Power factor	0.85
Inertia constant (M)	8MJ/MVA
Damping constant (D)	0.0
Stator leakage reactance	0.16

<u>d- axis</u>

Transient short circuit time constant (T'_{do})	5.044 sec
Transient reactance (X'_d)	0.3
Synchronous reactance (X_d)	1.0

<u>q- axis</u>

Synchronous reactance (X_q)	0.6

Excitation system data:

K_a=50 T_a=0.02 sec

Transformers data:

Leakage reactance   12.5

Transformer losses are negligible

* All dimensions are in p.u except indicated.

APPENDIX – III
System Matrices

$$A = \begin{bmatrix} 0 & \omega_b & 0 & 0 & 0 \\ -\dfrac{K_1}{M} & -\dfrac{D}{M} & -\dfrac{K_2}{M} & 0 & -\dfrac{K_{pdc}}{M} \\ -\dfrac{K_3}{T'_{do}} & 0 & -\dfrac{K_4}{T'_{do}} & \dfrac{1}{T'_{do}} & -\dfrac{K_{qdc}}{T'_{do}} \\ -\dfrac{K_5 K_a}{T_a} & 0 & -\dfrac{K_6 K_a}{T_a} & -\dfrac{1}{T_a} & -\dfrac{K_{vdc}}{T_a} \\ K_7 & 0 & K_8 & 0 & K_9 \end{bmatrix}$$

$$B = \begin{bmatrix} 0 & 0 \\ -\dfrac{K_{pm}}{M} & -\dfrac{K_{p\delta b}}{M} \\ -\dfrac{K_{qm}}{T'_{do}} & -\dfrac{K_{q\delta b}}{T'_{do}} \\ -\dfrac{K_{vm}.K_a}{T_a} & -\dfrac{K_{v\delta b}.K_a}{T_a} \\ K_{10} & K_{11} \end{bmatrix}$$

$$A_m = \begin{bmatrix} 0 & \omega_b & 0 & 0 & 0 \\ -\dfrac{K_1}{M} & -\dfrac{D}{M} & -\dfrac{K_2}{M} & 0 & -\dfrac{K_{pdc}}{M} \\ -\dfrac{K_3}{T'_{do}} & 0 & -\dfrac{K_4}{T'_{do}} & \dfrac{1}{T'_{do}} & -\dfrac{K_{qdc}}{T'_{do}} \\ -\dfrac{K_5 K_a}{T_a} & 0 & -\dfrac{K_6 K_a}{T_a} & -\dfrac{1}{T_a} & -\dfrac{K_{vdc}}{T_a} \\ K_7 & 0 & K_8 & 0 & K_9 \end{bmatrix}$$

59

$$A_{\delta b} = \begin{bmatrix} 0 & \omega_b & 0 & 0 & 0 \\ -\dfrac{K_1}{M} & -\dfrac{D}{M} & -\dfrac{K_2}{M} & 0 & -\dfrac{K_{pdc}}{M} \\ -\dfrac{K_3}{T'_{do}} & 0 & -\dfrac{K_4}{T'_{do}} & \dfrac{1}{T'_{do}} & -\dfrac{K_{qdc}}{T'_{do}} \\ -\dfrac{K_5 K_a}{T_a} & 0 & -\dfrac{K_6 K_a}{T_a} & -\dfrac{1}{T_a} & -\dfrac{K_{vdc}}{T_a} \\ K_7 & 0 & K_8 & 0 & K_9 \end{bmatrix}$$

$$B_{\delta b} = \begin{bmatrix} 0 \\ -\dfrac{K_{p\delta b}}{M} \\ -\dfrac{K_{q\delta b}}{T'_{do}} \\ -\dfrac{K_{v\delta b} \cdot K_a}{T_a} \\ K_{11} \end{bmatrix}$$

APPENDIX-IV

Constants of Modified Hefron-Phillips Model

The constants of Hefron –Phillips model are calculated from the expressions given below

$$K_1 = \frac{V_b \sin \delta_o .(X_d - X'_d) i_{qo}}{X_{2\Sigma}} + \frac{V_b \cos \delta_o .(E'_{qo} + i_{do} .(X_d - X'_d))}{X_{1\Sigma}}$$

$$K_2 = \frac{i_{qo} .(X_t + X_b + X_{sct} + X_d)}{X_{2\Sigma}}$$

$$K_{pdc} = \frac{m_o k \cos \delta_{bo}}{X_{1\Sigma}} .(E'_{qo} + i_{do} .(X_d - X'_d)) - \frac{m_o k \sin \delta_{bo}}{X_{2\Sigma}} .i_{qo} .(X_d - X'_d)$$

$$K_{pm} = \frac{k V_{dco} \cos \delta_{bo}}{X_{1\Sigma}} .(E'_{qo} + i_{do} .(X_d - X'_d)) - \frac{V_{dco} k \sin \delta_{bo}}{X_{2\Sigma}} .i_{qo} .(X_d - X'_d)$$

$$K_{p\delta b} = -\frac{m_o k V_{dco} \sin \delta_{bo}}{X_{1\Sigma}} .(E'_{qo} + i_{do} .(X_d - X'_d)) - \frac{m_o V_{dco} k \sin \delta_{bo}}{X_{2\Sigma}} .i_{qo} .(X_d - X'_d)$$

$$K_3 = \frac{V_b \sin \delta_o (X_d - X'_d)}{X_{2\Sigma}}$$

$$K_4 = \frac{(X_t + X_b + X_{sct} + X_d)}{X_{2\Sigma}}$$

$$K_{qdc} = -\frac{m_o k \sin \delta_{bo}}{X_{2\Sigma}} .(X_d - X'_d)$$

$$K_{qm} = \frac{V_{dco} k \sin \delta_{bo}}{X_{2\Sigma}} .i_{qo} .(X_d - X'_d)$$

$$K_{q\delta b} = -\frac{m_o V_{dco} k \cos \delta_{bo}}{X_{2\Sigma}} .(X_d - X'_d)$$

$$K_5 = X_q{}^2 .i_{qo} . \frac{V_b \cos \delta_o}{X_{1\Sigma}} - \frac{V_b \sin \delta_o}{X_{2\Sigma}} .X'_d .(E_{qo} - X'_d i_{do})$$

$$K_6 = (E_{qo} - X'_d i_{do}) . \frac{(X_t + X_b + X_{sct})}{X_{2\Sigma}}$$

$$K_{vdc} = X_q{}^2 .i_{qo} . \frac{m_o k \cos \delta_{bo}}{X_{1\Sigma}} + \frac{m_o k \sin \delta_{bo}}{X_{2\Sigma}} .X'_d .(E_{qo} - X'_d i_{do})$$

$$K_{vm} = X_q^2 . i_{qo} . \frac{V_{dco} k \cos \delta_{bo}}{X_{1\Sigma}} + \frac{V_{dco} k \sin \delta_{bo}}{X_{2\Sigma}} . X_d' . (E_{qo} - X_d' i_{do})$$

$$K_{v\ddot{o}b} = -X_q^2 . i_{qo} . \frac{m_o k V_{dco} \sin \delta_{bo}}{X_{1\Sigma}} + \frac{m_o k V_{dco} \cos \delta_{bo}}{X_{2\Sigma}} . X_d' . (E_{qo} - X_d' i_{do})$$

$$K_7 = \frac{m_o k V_b}{2C_{dc}} \sin (2\delta_{bo}) . [\frac{1}{X_{1\Sigma}} - \frac{1}{X_{2\Sigma}}]$$

$$K_8 = \frac{m_o k V_b}{C_{dc}} \frac{\cos (\delta_{bo})}{X_{2\Sigma}}$$

$$K_9 = \frac{m_o k}{2C_{dc}} \sin (2\delta_{bo}) . \left[\frac{1}{X_{1\Sigma}} - \frac{1}{X_{2\Sigma}} \right]$$

$$K_{10} = \frac{V_{dco} k}{2C_{dc}} \sin (2\delta_{bo}) . \left[\frac{1}{X_{1\Sigma}} - \frac{1}{X_{2\Sigma}} \right] + i_{do} . \cos \delta_{bo} + i_{qo} \sin \delta_{bo}$$

$$K_{11} = -\frac{m_o V_{dco} k}{2C_{dc}} \left[\frac{\cos^2 \delta_{bo}}{X_{2\Sigma}} . + \frac{\sin^2 \delta_{bo}}{X_{1\Sigma}} \right] + i_{qo} . \cos \delta_{bo} - i_{do} \sin \delta_{bo}$$

$$X_{1\Sigma} = X_t + X_b + X_l + X_q$$
$$X_{2\Sigma} = X_t + X_b + X_l + X_d'$$